Enclosure #1 1
Final Technical Report
USAF GR AFOSR 91-0333

Journal of Computational Neuroscience, X, 000-000 (1995).

Rhythmically Firing (20 - 50 Hz) Neurons in Monkey Primary Somatosensory Cortex: Activity Patterns During Initiation of Vibratory-Cued Hand Movements

MICHAEL A. LEBEDEV
RANDALL J. NELSON RNELSON@UTMEM1.UTMEM.EDU
Department of Anatomy and Neurobiology, University of Tennessee, Memphis, 875 Monroe Ave, Memphis, TN 38163, USA, telephone (901) 448 5979, fax (901) 448 7193

Received October 3, 1994; Revised April 27 1995, June 26, 1995; Accepted June 26, 1995

Action Editor: Eberhard Fetz

RA: Lebedev and Nelson
RT: Rhythmically Firing SI Neurons During Vibratory-Cued Movements
Keywords: somatosensory cortex, neuronal activity, rhythmic firing, hand movement, monkey, vibration.

Abstract. The activity patterns of rhythmically firing neurons in monkey primary somatosensory cortex (SI) were studied during trained wrist movements that were performed in response to palmar vibration. Of 1,222 neurons extracellularly recorded in SI, 129 cells (~11%) discharged rhythmically (at ~30 Hz) during maintained wrist position. During the initiation of vibratory-cued movements, neuronal activity usually decreased at ~25 ms after vibration onset followed by an additional decrease in activity at ~60 ms prior to movement onset. Rhythmically firing neurons are not likely to be integrate-and-fire neurons because, during activity changes, their rhythmic firing pattern was disrupted rather than modulated. The activity pattern of rhythmically firing neurons was complimentary to that of quickly adapting SI neurons recorded during the performance of this task (Nelson et al., 1991). Moreover, disruptions of rhythmic activity of individual SI neurons were similar to those reported previously for local field potential (LFP) oscillations in sensorimotor cortex during trained movements (Sanes and Donoghue, 1993). However, rhythmic activity of SI neurons did not wax and wane like LFP oscillations (Murthy and Fetz, 1992; Sanes and Donoghue, 1993). It has been suggested that fast (20 - 50 Hz) cortical oscillations may be initiated by inhibitory interneurons (Cowan and Wilson, 1994; Llinas et al., 1991; Stern and Wilson, 1994). We suggest that rhythmically firing neurons may tonically inhibit quickly adapting neurons and release them from the inhibition at go-cue onsets and prior to voluntary movements. It is possible that rhythmically active neurons may evoke intermittent oscillations in other cortical neurons and thus regulate cortical population oscillations.

Introduction

During the execution of motor tasks, large groups of sensorimotor cortical neurons intermittently become involved in coherent rhythmic activity (Murthy and Fetz, 1992; Sanes and Donoghue, 1993). Rhythmic activity has been suggested to be a functionally important type of neuronal firing that may serve to switch between behavioral modes and to establish dynamic coupling between cortical areas (for review, see Gray, 1994; Llinas, 1990; Lopes da Silva, 1991; Sheer, 1989; Singer, 1993; Steriade, 1993). Rhythmic activity in the form of local field potential (LFP) oscillations at ~40 Hz has been studied most extensively in cat visual cortex (Eckhorn et al., 1988; Gray and Singer, 1989; for review, see Engel et al., 1992; Gray et al., 1991; Gray, 1994; Singer, 1993). Similar LFP oscillations have been demonstrated in sensorimotor cortex in cat (Bouyer et al., 1981, 1987) and in monkey (Murthy and Fetz, 1992; Rougeul et al., 1979; Sanes and Donoghue, 1993). In these studies, it was suggested that oscillations in motor and sensory cortical areas play a role during behavior in sensorimotor integration and focal attention.

Individual neurons having oscillatory properties may be important for the initiation of cortical oscillations (Llinas, 1990; Steriade, 1993). Single morphologically identified neurons with 40-Hz rhythmicity, probably inhibitory interneurons, have been recorded in cortical slice preparations (Llinas et al., 1991). The presence of fast (~40 Hz) rhythmic IPSPs has been demonstrated while recording from pyramidal cortical neurons *in vivo* in urethane-anesthetized rats (Cowan and Wilson, 1994; Stern and Wilson, 1994). These rhythmic IPSPs may have resulted from cortical interneuronal inputs. In addition, depolarization-induced 20- to 40-Hz oscillations have been reported for a subset of cortical neurons with long axons recorded *in vivo* in urethane-anesthetized cats (Nuñez et al., 1992). Therefore, both intrinsic properties and extrinsic circuitry may be involved in generating rhythmic activity.

While the majority of data demonstrating oscillations in sensorimotor cortical areas has been obtained while recording LFPs during behavior (Bouyer et al., 1981; 1987; Murthy and Fetz, 1992; Rougeul et al., 1979; Sanes and Donoghue, 1993), some studies have examined rhythmic activity of single neurons. Murthy and Fetz (1994) described monkey sensorimotor cortical neurons that intermittently generated rhythmic discharges during episodes of LFP oscillations. Ahissar and Vaadia (1990) reported that second somatosensory cortical (SII) neurons recorded in awake monkeys often exhibited rhythmic activity that was sustained during immobility. The pattern of rhythmic firing of these SII neurons was disrupted by tactile stimulation or during voluntary movements. Ahissar and Vaadia (1990) suggested that oscillatory activity of SII neurons may be important for texture analysis. The functional role of rhythmically active neurons in the primary somatosensory cortex (SI) of behaving animals is not completely understood.

To determine the changes in activity patterns of rhythmically firing SI neurons during the initiation of somatosensory-cued movements, we analyzed data from experiments in which monkeys performed voluntary wrist flexions and extensions in response to vibrotactile go-cues. We examined the characteristics of rhythmic spike trains during a period when vibration was not present as well as how these spike trains changed in association with the presentation of vibrotactile go-cues and movement initiation. Also, we sought to relate the activity of rhythmically firing neurons with that of other SI neurons recorded during the same experimental paradigm (Nelson, 1988; Nelson et al., 1991; Lebedev et al., 1994). Based on these observations, we constructed a model depicting how rhythmically firing neurons may influence the firing patterns of other cortical neurons. Some of the data have been presented previously in preliminary form (Lebedev and Nelson, 1993).

Methods

Experimental Apparatus and Behavioral Paradigm

Six adult male rhesus monkeys (*Macaca mulatta*; monkeys C, F, G, H, M, and N) were trained to perform sensory-triggered wrist movements. The monkeys were cared for in accordance with the *NIH Guide for Care and Use of Laboratory Animals,* revised 1985. Each animal sat in an acrylic monkey chair with its right forearm on an armrest and its right palm on a moveable aluminum plate (Fig. 1A). One end of the plate was attached to the axle of a brushless DC torque motor (Colburn and Evarts, 1978). A load of 0.07 Nm was applied to the plate, which assisted wrist extensions and opposed flexions. Thus, to maintain a centered wrist position, the monkeys had to maintain pressure upon the plate using the palmar surface of their hands. Feedback of wrist position was provided by a visual display located 35 cm in front of the animals. This display consisted of 31 light-emitting diodes (LEDs) (Fig. 1B). Current wrist position was indicated by illuminating one of the LEDs. The middle, red, LED corresponded to a centered wrist position. Yellow LEDs above and below the middle LED indicated successive angular deviations of 1°.

Each monkey was trained to make untargeted ballistic wrist flexions or extensions in response to vibrotactile stimulation of their palms through the plate (Nelson, 1988; Nelson et al., 1991). Movements were executed by the same hand that was stimulated. The experimental paradigm is illustrated in Fig. 1C. To begin a trial, the monkey first centered the plate. At this time, a movement direction request was given by the presence or absence of illumination of an instructional red LED. This LED was located in the upper left corner of the visual display (Fig.

1B). Illumination of this LED signaled that extension was the appropriate movement. If this LED was not illuminated, the appropriate movement was flexion. The monkey was required to hold the plate in the centered position for 0.5, 1.0, 1.5, or 2.0 s (pseudorandomized). Movements of more than 0.5° from the center during this hold period canceled the trial. After the monkey successfully completed the hold period, the plate was vibrated by driving the torque motor with a sine wave at 27, 57 or 127 Hz. The angular deflection of the handle during the vibration was less than 0.06°. The onset of vibratory stimulation thus served as a cue for movement. When a movement of at least 5° in the required direction was made, the vibration was turned off, and the animal received a fruit juice reward. A new trial began when the animal once again centered the plate.

Electrophysiological Recordings and Histology

Once an animal achieved stable performance in the task (~2,000 rewarded trials per experimental session), a stainless steel recording chamber was surgically implanted over the skull to allow for extracellular recordings of the activity of SI neurons (see Nelson et al., 1991, for details). Transdural penetrations were made daily into the region of SI that represented the contralateral hand. Platinum-iridium microelectrodes with impedances of 1 - 2 MOhms were used for recordings. The depth of the electrode was varied to achieve the best isolation between the neuronal waveform in question and other visible neuronal activity. The activity of single units was amplified and discriminated using a time window discriminator having two independently controllable window thresholds. Each channel (upper and lower window) of the discriminator was armed by a waveform's first crossing of that threshold. An acceptance pulse of 0.2 ms was issued when that threshold was recrossed. The time from initial threshold crossing to the end of the acceptance pulse was typically on the order of 0.5 ms. As well, the electronic refractory period of the entire data collection system while running the paradigm was confirmed to be on the order of 0.4 ms by analyzing recordings of white noise. Pulse data was stored in a computer by conventional means (Evarts, 1966; Lemon, 1984).

Neuronal receptive fields (RFs) were manually examined outside the task by lightly touching skin surfaces with hand-held probes, manipulating joints, and palpating muscles. An RF was classified as "cutaneous" if the neuron preferentially responded to light touch, and as "deep" if the neuron responded to bending a joint or to muscle palpation. To ensure that stimulation of overlying skin was not mistaken as a response from a muscle, the skin was displaced laterally and the muscle again palpated. For some neurons, no clear RF could be found.

At regular intervals, the EMG activity of forearm muscles acting across the wrist was recorded (Nelson, 1987). Intramuscular EMG wires (stranded stainless steel, TEFLON® insulated; Bergen Wire Rope Co.) were temporarily implanted in muscles by using sterile 25-gauge needles as guides. EMG activity was converted into pulse data with a window discriminator (Vaadia et al., 1988; Lebedev et al., 1994) and stored in the same form as the neuronal data.

On the last recording day, electrolytic lesions (10 μA of current for 10-20 s) were made in the cortex to mark locations of interest. The animals were then deeply anesthetized with sodium pentobarbital and transcardially perfused with 10% buffered formol-saline. Histological sagittal sections of the cortex were prepared, and recording sites were reconstructed based upon the depth of each electrode penetration and its location with respect to the marking lesions (Fig. 2) (Nelson, 1988; Nelson et al., 1991).

Analyses of Rhythmic Spike Trains

Rhythmically firing SI neurons were selected by examining the 500-ms epoch of the spike trains that immediately preceded vibration onset. This corresponded to the shortest duration of the hold period during which an animal actively maintained a stable wrist position. Because of this time limit, slow rhythmic activity (< 8 Hz) could not be detected. Conclusions on whether neurons fired rhythmically or nonrhythmically were made by examining the expectation density (ED)

histograms (Mountcastle et al., 1969, 1990). ED, also termed the "autocorrelation function" (Zadeh, 1957), represents the probability of a neuronal discharge at a certain time after a given discharge. For rhythmic spike trains, ED histograms contain peaks at the multiples of the rhythmic period (Fig. 3A) (Perkel et al., 1967; Poggio and Viernstein, 1964; Segundo et al., 1968). The average height of subsequent bins in the ED histogram gradually flattens to a stabilized level (Fig. 3A). We quantified the degree of rhythmicity as the ratio of the height of the first ED peak to the stabilized level of ED histogram:

$$E'_1 = E_1 / R, \quad (1)$$

where E'_1 is the normalized height of the first peak measured from zero level, E_1 is the height of the first peak, and R is the stabilized level. The stabilized level was calculated by averaging ED bins in the range 0 to 200 ms.

The selection of rhythmically firing neurons was made using four criteria: (1) mean firing rate of the selected neurons during the hold phase of the paradigm exceeded 10 spikes/s; (2 and 3) the heights of the first and second ED peaks were greater than $1.5R$ and $1.2R$, respectively (Fig. 3C, D); (4) time intervals from zero to the first peak (t_1, Fig. 3A) and from the first to the second peak ($t_2 - t_1$) differed by less than 15% (percentage Jitter, Fig. 3D). Criterion 1 was used to initially select the population of tonically active neurons. Criterion 2 was chosen because the distribution of E'_1 for tonically active neurons indicated a major subpopulation with E'_1 in the range of nonrhythmic firing (1 - ~1.5) and a smaller subpopulation of the neurons with $E'_1 > 1.5$ (Fig. 3B - D). Criteria 3 and 4 previously have been used by Ahissar and Vaadia (1990) and confirmed the presence of multiple peaks in ED histogram. The distributions of E'_1 for the selected groups of rhythmically and nonrhythmically firing neurons were statistically different ($p < 0.0001$; unpaired t-test), and had a small overlap in the range of E'_1 from 1.5 to ~2.0 (Fig. 3B). For rhythmically active neurons, their rhythmic frequency was calculated as

$$f = 2 / [t_1 + (t_2 - t_1)], \quad (2)$$

where f is rhythmic frequency and t_1, t_2 are the intervals from zero to the first and second peaks, respectively. Some ED histograms showed qualitative features that were characteristic of bursty activity pattern (Wilson et al., 1977; Wilson and Groves, 1981). These ED histograms indicated high probability of firing at very short intervals after spike generation (<10 ms). Firing probability then decayed gradually to the stabilized level over a period of 20 - 50 ms. Bursty neurons were excluded from these analyses.

Renewal density (RD) histograms and joint interval plots were calculated to determine the degree of serial dependency in the spike trains. We sought to determine whether the rhythmic spike sequences of SI neurons were reset after the occurrence of each discharge (that is, could be described as a renewal process) (Perkel et al., 1967) or more complex serial dependencies of the ISIs were present. Nonrenewal spike trains often occur when a neuron is rhythmically driven by external inputs (Mountcastle et al., 1969, 1990; Surmeier and Towe, 1987a, 1987b). Joint interval scattergrams display each ISI as a function of its immediately preceding ISI (Fig. 4B). Joint interval methods have been used to analyze serial dependencies of the ISIs (Rodieck et al., 1962; Surmeier and Towe, 1987a, 1987b; Siebler et al., 1991). Another technique for detecting serial dependencies of the ISIs is the RD method (Mountcastle et al., 1969, 1990; Perkel et al., 1967; Poggio and Viernstein, 1964). RD is the ED calculated for randomly shuffled ISI sequences (Fig. 4D, E). For a simple renewal process, ED and RD histograms are not different. However, if serial dependencies of the ISIs are present, these histograms may be different. Thus, in the case of externally driven activity, a peak in a RD histogram is smaller than the corresponding peak in the ED histogram (Mountcastle et al., 1969, 1990). To estimate the difference between ED and RD histograms, we compared the magnitudes of the first and second peaks in the ED histogram normalized by the stabilized level with those of corresponding peaks in the RD histogram.

Analyses of Changes in Neuronal Activity and EMG

Changes in neuronal activity associated with go-cues and movements were analyzed using conventional discharge histograms (Fig. 5B) and raster displays (Fig. 5C). In addition, ISI rasters

were plotted that displayed the time of occurrence of each spike on the x-axis and the succeeding ISI on the y-axis (Fig. 5A). To analyze vibration-related changes in activity, the occurrences of individual discharges were expressed as times with respect to vibration onset (Fig. 5A - E, left panels). For the analysis of movement-related changes, spike occurrences were expressed with respect to movement onset (Fig. 5A - E, right panels).

The onsets of changes in neuronal firing rate and of changes in EMG were determined using the cumulative sum methods (CUSUM) (Ellaway, 1977; Jiang et al., 1991). The CUSUM at a given time is the total number of discharges accumulated for all trials from some starting time. The average CUSUM was calculated by rescaling this count by dividing it by the number of trials (Fig. 5D). The CUSUM for an impulse train for which the probability of discharge is constant over time is a linearly rising curve with a slope equal to the mean firing rate. To calculate the onset of deviations from the stationary level of activity, the largest epoch of linear rise in the average CUSUM prior to a behaviorally significant event was labeled by visual inspection. A linear least-squares interpolation curve was calculated for this period. This curve was then extrapolated through the epoch containing the event. The standard deviation of the CUSUM from the fitted curve was calculated for the epoch that had a linear rise. The computer program searched forward in time to find the first change in the CUSUM from the curve of more than three standard deviations for at least 40 ms. This time was designated as the onset of a significant change in activity.

The correlation between the periodic vibratory stimulus and neuronal discharges was analyzed using a phase representation method (for details, see Lebedev et al., 1994). The phase of each spike with respect to the stimulus cycle was calculated and plotted in a scattergram as a function of time (see, e.g., Fig. 8B). In addition, the phase relative to the extrapolated stimulus sinusoid was automatically calculated by the computer for the epoch preceding vibration onset. For this epoch, phase was randomly scattered. Following vibration onset, if the activity was entrained to the stimulus, a band was present in the phase scattergram that corresponded to the phase of preferential response. Cycle distribution histograms also were calculated that represented the probability of discharge occurrence in relationship to the phase of the stimulus cycle (see, e.g., Fig. 8G).

Statistical Analyses

The characteristics of neuronal activity for several groups of neurons (having specific RF types, located in given cortical areas, and so on) were statistically compared using a multifactorial ANOVA (with the Scheffé post hoc test). The parametric *t*-test and the more robust nonparametric Mann-Whitney *U*-test were used for two group comparisons.

Results

Cortical Locations and Receptive Fields

Of the total recorded 1,222 SI neurons, 706 (~58%) neurons had firing rates of more than 10 spikes/s during the hold period of the paradigm. Of this sample, 70/706 (~10 %) neurons exhibited bursty firing patterns and were excluded. Eight of the remaining 636 neurons, were excluded from consideration because they had either a small number of ISIs shorter than 1ms (approximately twice the spike duration) or inconsistent activity patterns during the experimental session. Either occurrence could indicate inclusion in the records of spikes from another nearby neuron. Thus, 129/1222 neurons (~11%) having rhythmic activity patterns were selected (Fig. 3B). The distribution of surface locations of the recording sites and their location in representative sagittal sections are shown in Fig. 2C. No clear distribution patterns were evident, either within or across cortical areas (areas 3a, 3b, 1, and 2). Ninety-one neurons were tested for RFs. This sample contained more neurons with deep RFs than those with cutaneous RFs or no clear RF (Fig. 2B). Cutaneous RFs most frequently were associated with palmar surface of the hand. Deep RFs were associated with movements of fingers and the wrist or with deep hand tissues.

Characteristics of Rhythmic Activity

The activity of rhythmically firing neurons that occurred during the hold period was analyzed to determine its frequency characteristics as well as any serial dependencies of the ISIs. An example of spike train analyses for an area 1 neuron is presented in Fig. 4. The activity of the same neuron during task execution is illustrated in Fig. 5. In Fig. 4A, a scattergram of ISIs during a 500-ms epoch preceding vibration onset is plotted for 40 consecutive trials. This scattergram shows that the ISI distribution remained virtually unchanged from trial to trial. In Fig. 4B, a joint interval scattergram is presented. Fig. 4C, D, and E display ISI distribution, ED, and RD histograms, respectively. During the hold period, this neuron was rhythmically active at ~39 Hz. The majority of ISIs were distributed within the range of ± 5 ms around the rhythmic period (~25.6 ms). Note, however, that a small number of outlying short and long ISIs occurred. ED and RD histograms were not substantially different.

Statistical analyses of the first normalized ED peaks (E'_1, equation 1) and the rhythmic frequencies (f ; equation 2) for the sample of rhythmically active neurons did not show any significant differences depending on cortical location of the neurons nor on their RF type. The means and the standard deviations were, for E'_1, 2.62 ± 0.78 (Fig. 3B) and, for f, 32.1 ± 5.4 Hz (Fig. 3E).

We observed two features of spike trains that seem unlikely for a renewal model of rhythm generation (Perkel et al., 1967). These features were (1) multimodal ISI distributions and (2) the occurrence of a small but noticeable number of ISIs at less than the modal interval that formed diagonal bands in joint interval scattergrams. Multimodal ISI distributions were observed for 31/129 neurons (~24%). An example of an area 1 neuron with a multimodal ISI distribution is presented in Fig. 6A-D (also see Figs. 9 and 11). The ISI distribution of this neuron contained peaks at the modal interval (T) and at twice that interval ($2T$, Fig. 6B). The joint interval scattergram for this neuron had four clusters of ISIs pairs around points (T, T), (T, $2T$), ($2T$, T), and ($2T$, $2T$). ED and RD histograms were approximately the same for this neuron. For 32/129 neurons (~25%), we observed the occurrence of ISIs that were shorter than modal interval. Six neurons (~5%) exhibited both these short ISIs and multimodal ISIs. Short ISIs that form diagonal bands in joint interval plots have been attributed to "interrupting spikes" (Surmeier and Towe, 1987a, 1987b; Siebler et al., 1991). Joint interval scattergrams for such spike trains contain diagonal bands that connect points (0, T) and (T, 0). These bands occur when the sum of the ISIs that immediately precede and succeed the interrupting spikes is equal to the modal interval:

$$T_1 + T_2 = T, \qquad (3)$$

where T_1 is the ISI preceding an interrupting spike and T_2 is the succeeding ISI. Records for an area 3b neuron that exhibited interrupting spikes are presented in Fig. 6E - H. In addition to a cluster of ISIs around T, shorter ISIs were present (from 2 ms to T, Fig. 6F). In the joint interval scattergram, the presence of short intervals resulted in a diagonal band. Note that peaks in the RD histogram were less pronounced than those in the ED histogram.

The comparison of ED and RD histograms for the total sample of rhythmically firing cells showed a tendency for peaks in RD histograms to be smaller in amplitude than those in ED histograms. The results of a factorial ANOVA indicated that, for the neurons having interrupting spikes, the differences between ED and RD peaks were significantly greater compared with the rest of the total sample. For these neurons, the means and standard deviations of the differences between the first two ED and RD peaks were 13.4 ± 9.7% and 13.8 ± 9.2%, respectively ($p <$ 0.0002; paired t-test). When the neurons with interrupting spikes were excluded from the total sample, a small but statistically significant difference was found only for the first peaks (1.8 ± 5.0%; $p < 0.0002$).

Vibration-Related Activity

Changes in the activity of SI neurons in this experimental paradigm commonly occurred at

vibratory go-cue onset and often preceded movement onset (Nelson, 1988). We analyzed the changes in activity of rhythmically firing neurons that occurred in association with these behaviorally significant events. For 67/129 rhythmically active neurons (~52%), the firing rate changed with vibration onset. Decreases in activity were the most common responses to vibration (60/67 cases, ~89%). An example of a typical response to vibration exhibited by an area 1 neuron is presented in Fig. 7A. The neuron's firing rate decreased following palmar vibration with a latency of ~28 ms. The vibration-related activity decrease consisted of both transient and sustained changes in activity (schematic illustration, Fig. 7E). The analyses of the latency of vibratory responses are presented in Fig. 7F. This latency (~26 ms at 57 Hz) was not significantly different as a function of cortical location or RF type.

In some cases, neuronal activity during ongoing vibration, although decreased, was stimulus-entrained. An example of an area 3a neuron with activity entrained to a 27 Hz vibratory stimulus is presented in Fig. 8. During the hold period, the neuron was rhythmically active at ~30 Hz. A transient decrease in activity occurred at ~27 ms after vibration onset and lasted for ~50 ms (Fig. 8A). Then, the activity recovered, although it was at a lower level than that during the hold period. Moreover, neuronal discharges were entrained to the ongoing 27 Hz vibration. The entrainment is clearly seen in phase raster (Fig. 8B) and in the cycle distribution histogram (Fig. 8G). The ISI distribution for the epoch of vibratory stimulation contained peaks at the vibratory period and at twice that period (Fig. 8F). Generally, entrainment was observed more often when stimulating at 27 Hz, which was close to the average rhythmic frequency of the studied neurons. Of 41 neurons recorded during stimulating at this frequency, 12 neurons (~29%) exhibited vibration-entrained activity. The majority of the data were collected while stimulating at 57 Hz. At this frequency, 12/129 neurons (~9%) exhibited vibratory entrainment. At the highest stimulus frequency (127 Hz), vibratory entrainment rarely was observed (1/38; ~3%).

Premovement Activity

The activity of each rhythmically firing neuron changed prior to movement onset for at least one movement direction. The earliest change of firing rate from the stabilized level of activity during vibratory stimulation was designated as the onset of premovement activity (PMA) (Nelson, 1988). PMA was detected in 124/129 instances for flexion movements and in 118/129 instances for extension movements. Decrease in firing rate was the most frequent type of PMA (~76% of PMA cases; Fig. 9F). Figure 9A illustrates this pattern. Records for an area 2 neuron are presented. The firing rate of this neuron did not change after vibration onset. However, its activity was dramatically decreased at ~40 ms prior to the onset of extension movements. The PMA onsets with respect to movement onset were not statistically different as a function of cortical location or RF type. These onsets also did not differ between instances of activity increases and decreases.

To estimate the temporal relationship between PMA and the earliest movement-related peripheral afferent signals, PMA onsets were compared with EMG onsets. The EMG onsets were analyzed for several forearm and arm muscles (Lebedev et al., 1994; Nelson, 1987; Nelson et al., 1991). A minimal afferent peripheral conduction time of 11 ms was subtracted from the actual EMG onsets (Wiesendanger and Miles, 1982) to yield an estimate of the time at which afferent signals resulting from muscle activity might reach the cortex. The earliest time at which this might occur was thus 100 ms prior to movement onset, whereas given the average EMG onset, it was 60 ms prior to movement onset. A substantial number of PMA onsets for rhythmically firing neurons occurred after the earliest estimated time of afferent input arrival (194/242; ~80%) (Fig. 9F). Many PMA onsets occurred after the average estimated time of afferent input arrival (133/242; ~55%).

During activity decreases, rhythmic activity often was disrupted rather than modulated (e.g., Fig 9A). In the cases when the rhythmic pattern of discharges was preserved, the rhythmic frequency decreased slightly (by ~20%; e.g., sustained vibratory response in Fig. 5A). Activity increases usually occurred *during* movements and were characterized by transitions from rhythmic to nonrhythmic firing. In Fig. 10, records for an area 1 neuron are presented that show activation during voluntary extensions. This neuron also was activated by passive extension of the second digit at the metacarpophalangeal joint (Fig. 10B). Rhythmic firing decreased at ~27 ms following vibration onset and, additionally, at ~34 ms prior to extension movement onset. Then, a

pronounced activation followed at ~45 ms after movement onset. This activation was characterized by a qualitative change in the ISI distribution (Fig. 10D and E). The ISI distribution shifted to the left, indicative of the faster firing rate. However, several ISIs occurred at the minimum value of 1.2 ms, possibly indicating the presence of small bursts of activity in this otherwise rhythmically spiking neuron. In some instances, transitions to irregular ISI patterns occurred without substantial changes in the mean firing rate (e.g., ~200 ms after movement onset in Fig. 6E and 11A).

Activity patterns were analyzed to determine if PMA types were dependent upon the direction of subsequent movement. If the sign of the activity change was opposite for flexion and extension or if PMA occurred only for one movement direction, this instance of PMA was classified as directional. If the activity change was of the same sign for both movement directions, the PMA was classified as nondirectional. Nondirectional PMA occurred most frequently (84/129 neurons, ~65%); directional PMA was observed for 45/129 neurons (~35%). An example of an area 3a neuron with a nondirectional PMA pattern is presented in Fig. 11. For both flexions (Fig. 11A) and extensions (Fig. 11D), premovement decreases in activity of this neuron occurred at ~70 ms prior to movement onset.

Comparison with Other SI Neurons

We compared the activity pattern exhibited by rhythmically firing neurons with the types of activity of SI neurons that have been documented previously for this experimental paradigm (Nelson, 1988; Nelson et al., 1991). The typical activity pattern of rhythmically firing neurons resembled a mirror image of the activity of quickly adapting (QA) neurons recorded during similar behaviors (Nelson et al., 1991). QA neurons were activated at about the same time following vibratory cue onset (~30 ms) and prior to movement (~80 ms) as the firing rate of rhythmically firing SI neurons decreased.

Discussion

Activity of Rhythmically Firing Neurons During Trained Motor Tasks

We examined the activity of a population of rhythmically firing neurons in monkey SI while the animals performed trained motor tasks. The changes in activity of these neurons had common features during the initiation of vibratory-cued movements. Approximately one-half of rhythmically firing neurons responded to vibratory go-cues, typically with decreases in firing rates at ~25 ms after vibration onset. In some cases, although the firing rate was decreased somewhat, the activity was entrained to the frequency of the ongoing vibration. It is possible that the entrainment observed was caused by IPSPs rather than by EPSPs (Cowan and Wilson, 1994; Lytton and Sejnowski, 1991; Stern and Wilson, 1994). The best vibratory frequency for this entrainment was close to the population's average frequency of rhythmic activity (~30 Hz). This observation is consistent with a model of texture perception proposed by Ahissar and Vaadia (1990). In this model, cortical oscillators are key elements in neuronal circuits that analyze the temporal properties of somatosensory discharges using a phase-locked loop algorithm (Horowitz and Hill, 1980). The model predicts that oscillatory neurons would follow somatosensory stimuli if the stimulus frequency is close to the frequency of spontaneous oscillations of these neurons. Although our experiments were not specifically designed to examine the role of rhythmically active neurons in somatosensory perception, our results generally support this prediction.

Decreases in the activity of rhythmically firing neurons often occurred at ~57 ms prior to movement onset. Thus, a typical activity pattern consisted of a decrease in firing rate after vibration onset and an additional decrease in firing rate prior to movement onset. This activity pattern is complementary to the pattern previously reported for QA neurons that were recorded during the performance of this behavioral task (Nelson et al., 1991). QA neurons exhibit a short-duration burst of spikes after vibration onset. Then their activity decreases and is reactivated prior to movement onset. Nelson et al. (1991) suggested that QA activity patterns may occur because of

gating of SI sensory responsiveness at behaviorally significant times. The function of gating may be to enhance sensory inputs that are important for the current behavioral task while suppressing others that are not (Chapin and Woodward, 1982; Chapman et al., 1988; Coquery, 1978; Dyhre-Poulsen, 1978; Nelson, 1988; Rushton et al., 1981). Because of the correspondence between the activity patterns of rhythmically firing and QA neurons, it seems reasonable to assume that rhythmically firing neurons may participate in gating SI activity.

Centrally generated as well as peripheral inputs to SI neurons may be involved in premovement gating of somatosensory activity (Chapin and Woodward, 1982; Chapman et al., 1988; Coquery, 1978; Dyhre-Poulsen, 1978; Lebedev et al., 1994; Nelson, 1987; Nelson et al., 1991; Soso and Fetz, 1980). Changes in the activity of rhythmically firing neurons that occurred before movement usually happened after the earliest EMG onset. Therefore, these changes certainly could be related to peripheral afferent signals associated with the onset of muscle activity that preceded movement onset as detected by the change in handle position. However, most premovement activity changes were of the same sign for both flexion and extension trials (that is, they were nondirectional). Peripheral reafferent signals commonly are directional, especially those of proprioceptive origin (Cohen et al., 1994; Soso and Fetz, 1980). Many of the rhythmically firing SI neurons in our sample had deep RFs. Nonetheless, they usually exhibited nondirectional premovement activity patterns. Therefore, the premovement changes in activity of rhythmically firing SI neurons probably are not simply replicas of peripheral reafferent signals but rather might reflect intracortical processing of peripheral information.

Rhythmically Active SI Neurons and LFP Oscillations

Our present observations suggest that there are similar features between the activity patterns of rhythmically firing SI neurons and the LFP oscillations in sensorimotor cortex reported by others. The mean firing frequency of the observed rhythmically firing SI neurons (~30 Hz) was close to the frequency often described for LFP oscillations (Bouyer et al., 1981, 1987; Murthy and Fetz, 1992; Rougeul et al., 1979; Sanes and Donoghue, 1993). In a manner similar to LFP oscillations, rhythmic activity of single SI neurons was disrupted with somatosensory stimulation and/or voluntary movements. LFP oscillations occur in sensorimotor cortex in the cat (Bouyer et al., 1981, 1987) and the monkey (Rougeul et al., 1979) during focused attention and immobility but usually disappear during movements. Disruptions of LFP oscillations in monkey motor cortex also occur prior to movements performed during trained motor tasks (Sanes and Donoghue, 1993). In addition, Murthy and Fetz (1992) observed that LFP oscillations in monkey motor and somatosensory cortices occurred *during* exploratory movements requiring directed attention. Thus, LFP oscillations may vary as a function of attentive behavior and task requirements (for review, see Gray, 1994). Experimental conditions of Sanes and Donoghue (1993) are the most similar to ours. Disruptions of LFP oscillations in their experiments occurred around the same time as the disruptions of rhythmic firing of individual SI neurons in our experiments. We suggest, therefore, that LFP oscillations and rhythmic firing of SI neurons may be related.

Some characteristics of rhythmic activity of individual neurons, however, differ from those reported for LFP oscillations. LFP oscillations usually occur as occasional rhythmic bursts, 100 - 200 ms in duration and often with a variable frequency from one burst to another (Eckhorn et al., 1988; Gray and Singer, 1989; Murthy and Fetz, 1992; Sanes and Donoghue, 1993; Singer, 1993). The activity patterns of individual rhythmically firing SI neurons were consistent from trial to trial and were only briefly interrupted during vibratory stimulation and movements. We suggest that individual rhythmically firing SI neurons may maintain relatively independent activity. Further, it is possible that these neurons may intermittently evoke oscillations in other neurons. Murthy and Fetz (1994) observed sensorimotor cortical neurons that intermittently exhibited episodes of rhythmic activity during episodes of LFP oscillations. These neurons could be driven by neurons with sustained rhythmic activity. Driven oscillations of cortical neurons may become synchronized through cortico-cortical and thalamocortical interactions (Llinas, 1990; Llinas et al., 1991). Thus, rhythmically firing neurons may act to regulate cortical population oscillations.

Possible Models of Rhythmic Activity

Mechanisms causing rhythmic activity of SI neurons remain unclear. One possibility is that rhythmically active cells are integrate-and-fire neurons, and their regular firing occurs because of stable synaptic input (Segundo et al., 1968). Regular spiking cortical pyramidal neurons discharge very rhythmically in an integrate-and-fire mode, when they receive steady inputs (McCormick et al., 1985; Softky and Koch, 1993). Integrate-and-fire neurons respond to changes in the intensity of synaptic input by changing their firing frequency. If rhythmically firing SI neurons are integrate-and-fire neurons activated by stable peripheral inputs, then their firing frequency should follow changes in the intensity of peripheral inputs, for example, as might occur during movements. However, the rhythmic firing of SI neurons is disrupted rather than being modulated during movements. Thus, modeling rhythmically firing neurons as integrate-and-fire neurons does not describe all of our observations.

Alternatively, rhythmic firing may result from extrinsic oscillatory drive. Rhythmic driving of cortical neurons produced by intracortical and/or subcortical inputs previously has been proposed. Ghose and Freeman (1992) suggested that visual cortical neurons may be driven by rhythmically active cells located in the lateral geniculate nucleus. Jagadeesh et al. (1992) demonstrated rhythmic excitatory inputs to visual cortical neurons using *in vivo* patch clamp recording techniques. The source of rhythmic drive may be from inhibitory, rather than excitatory, neurons (Cowan and Wilson, 1994; Llinas, 1990; Llinas et al., 1991). Some of our observations are consistent with an extrinsic drive model. We observed ISIs for some neurons that occurred at multiples of the modal interval. This may have occurred because of a neuron's occasional failures to respond to driving inputs as previously suggested (Ahissar and Vaadia, 1990). In addition, we observed interrupting spikes that may reflect spikes that are uncorrelated with the rhythmic drive (Surmeier and Towe, 1987a, 1987b). However, from the manner in which these neurons were recorded, we cannot absolutely eliminate the possibility that interrupting spikes or ISIs at multiples of the modal interval could reflect occasional spurious inclusion spikes from adjacent neurons with similar waveforms or exclusion of spikes from the neuron in question. Further experiments are required to clarify this issue.

Rhythmic driving of SI neurons could arise from regular discharges of peripheral afferents. Single peripheral afferent fibers may have very regular firing patterns (e.g., Burke et al., 1987). However, the frequency of rhythmic discharge of peripheral afferents is modulated during movements (Burke et al., 1987; Prochazka, 1985). Since rhythmic activity of SI neurons typically was disrupted periodically, these neurons were unlikely to be driven by peripheral afferent discharges throughout all phases of our behavioral task. Moreover, the SI neurons that seem to have been driven most securely by peripheral inputs did not exhibit rhythmic activity. These neurons which had cutaneous or deep RFs faithfully responded to vibratory go-cues with entrained discharges (Lebedev et al., 1994). However, they did not fire rhythmically during the hold period of the paradigm (unpublished observations). Therefore, it seems unlikely that peripheral drive is the major source of rhythmic firing of SI neurons under these experimental conditions.

Rhythmic activity of some of the studied neurons could be the result of intrinsic oscillatory properties rather than extrinsic factors. For many rhythmically firing neurons (72/129; ~56%) we did not observe signs of extrinsic drive (that is, interrupting spikes and multimodal distributions of the ISIs). Moreover, ED and RD histograms for these neurons were virtually identical. Mountcastle et al. (1969, 1990) reported that ED and RD histograms were dramatically different when the firing of SI neurons was driven by peripheral vibration. Absence of such differences between ED and RD histograms for many rhythmically active SI neurons may indicate either that these neurons were not extrinsically driven or that they were driven by very secure oscillatory inputs.

Intrinsically oscillating cortical neurons have been reported. Two types of neurons recorded *in vitro* have been demonstrated to intrinsically oscillate at 10 - 50 Hz within layer 4 of guinea pig frontal cortex (Llinas et al., 1991). Neurons of the first type - that is, broad-frequency oscillators - increased their firing frequency with membrane depolarization. Neurons of the second

type, the narrow-frequency oscillators showed little change in firing frequency as a function of the level of depolarization. The narrow-frequency oscillatory neurons have been identified morphologically as sparsely spinous interneurons having axon collaterals in layers 3 and 4, and are probably inhibitory interneurons. Pyramidal cortical neurons typically do not generate fast (20 - 50 Hz) oscillations intrinsically (Silva et al., 1991). Rather, their activity is thought to be modulated by rhythmic IPSPs probably generated by cortical interneurons (Cowan and Wilson, 1994; Stern and Wilson, 1994; but see also Nuñez et al.,1992). Thus observations tend to indicate that rhythmically firing neurons in the cortex may be inhibitory interneurons.

Rhythmically Active Neurons and Tonic Inhibition of SI Activity

Since cortical oscillatory neurons are likely to be inhibitory interneurons (Cowan and Wilson, 1994; Llinas et al., 1991; Stern and Wilson, 1994), there is the intriguing possibility that rhythmically active SI neurons may be involved in tonic inhibition of SI activity. The role of inhibitory interneurons as essential regulators of cortical activity is suggested by the observation that ~70% of intracortical connections are inhibitory (White, 1989). Tonic inhibition produced by local interneurons has been suggested to control RF size of cortical neurons and to increase spatial and temporal contrast (Brooks, 1959; Dykes et al., 1984). We further suggest that inhibitory interneurons may gate SI activity during behavior. The activity patterns of rhythmically firing neurons are complimentary to the activity patterns of quickly adapting (QA) neurons recorded during this behavior (Nelson et al., 1991). This observation is similar to that of Wilson et al. (1994), who observed that putative GABA-ergic interneurons and pyramidal neurons exhibited complementary patterns of activity while the monkeys performed visual and oculomotor tasks. These authors suggested that interneurons may hyperpolarize pyramidal neurons, whereas pyramidal neurons may depolarize interneurons. Similar reciprocal connections may be present between rhythmically firing and QA SI neurons.

Rhythmically firing neurons are candidates for one element of a model that was previously proposed to account for observed patterns of activity of QA SI neurons (Nelson et al., 1991). A task phase element was proposed that may suppress peripheral and motor inputs to QA neurons. In Fig. 12, a model is presented that is a modified form of the previous one. This model includes output neurons (such as corticocortical, corticothalamic or corticofugal), input neurons (presumably, layer IV spiny cells) (Jones, 1975) and two types of inhibitory interneurons, rhythmic and phasic interneurons. This model assumes the following functional relationships. Rhythmic interneurons exhibit sustained firing patterns, whereas phasic inhibitory interneurons respond to inputs with transient bursts of spikes. The model includes neurons that receive direct excitatory inputs from other regions. The model has been conceived such that rhythmically firing neurons tonically inhibit output neurons. Output neurons may be disinhibited because their inhibitors themselves receive inhibitory inputs from phasic interneurons. During increases in SI input, phasic inhibitory neurons would be transiently activated. Consequently, by this model, rhythmically firing neurons would be transiently inhibited. This scheme suggests that output neurons generate bursts of spikes when released from tonic inhibition and are excited by input signals. Quickly adapting activity patterns of output neurons may be important for signalling transient sensory events.

The model shown in Fig. 12 is consistent with the data on intracortical connectivity (Chagnac-Amitai and Connors, 1989; Istvan and Zarzecki, 1994; Jones, 1975). Nonpyramidal inhibitory neurons that may regulate activity of other cortical neurons previously have been studied (Kawaguchi, 1993; Kawaguchi and Kubota, 1993; Jones, 1975). One type of neuron, the double bouquet cell (Ramón y Cajal, 1911), has been shown to project to nonpyramidal cortical cells (Somogyi and Cowey, 1981). These cells are characterized by vertically oriented axonal arbors. Recent findings suggest that GABA-ergic cortical neurons with this type of axonal arbors are immunoreactive for calbindin-28, whereas GABA-ergic neurons with horizontally oriented axonal arbors (for example, the basket cells) are immunoreactive for parvalbumin (Hendry et al., 1989; Kawaguchi and Kubota, 1993). Moreover, calbindin-28-immunoreactive neurons respond to current injections by firing phasically, whereas parvalbumin-immunoreactive neurons respond by firing repetitively with little or no spike frequency adaptation (Kawaguchi and Kubota, 1993).

Therefore, calbindin-28 and parvalbumin-immunoreactive neurons are likely candidates for the phasic and rhythmic inhibitory elements of the model, respectively.

This model's circuitry may be capable of initiating network oscillations following the scheme proposed by Llinas et al. (1991). Rhythmically firing inhibitory neurons may induce rhythmic activity in output neurons. Output neurons, in turn, may induce rhythmic activity in their target regions, for example in the thalamus or in other cortical areas. Regions projecting back to the cortex would, thus, close the loop which would be necessary for the maintenance of network oscillations.

Acknowledgments

We thank J. M. Denton for technical assistance during the data collection and analysis, and D. L. Armbruster, D. J. Surmeier, C. J. Wilson, and P. Zarzecki for detailed comments on versions of this manuscript. This work was supported by United States Air Force Grant AFOSR 91-0333 to R. J. Nelson.

References

Ahissar E, Vaadia E (1990) Oscillatory activity of single units in a somatosensory cortex of an awake monkey and their possible role in texture analysis. Proc Natl Acad Sci USA 87: 8935 - 8939.

Bouyer JJ, Montaron MF, Rougeul A (1981) Fast fronto-parietal rhythms during combined focused attentive behavior and immobility in cat: Cortical and thalamic localizations. Electroenceph Clin Neurophysiol 51: 244 - 252.

Bouyer JJ, Montaron MF, Vahnee JM, Albert MP, Rougeul A (1987) Anatomical localization of cortical beta rhythms in cat. Neuroscience 22: 863 - 869.

Brooks VB (1959) Contrast and stability in the nervous system. Trans NY Acad Sci 21: 387 - 394.

Burke D, Gandevia SC, Macefield G (1987) Responses to passive movements of receptors in joint, skin and muscle of the human hand. J Physiol (London) 402: 347 - 361.

Chagnac-Amitai Y, Connors BW (1989) Synchronized excitation and inhibition driven by intrinsically bursting neurons in neocortex. J Neurophys 62: 1149 - 1162.

Chapin JK, Woodward DJ (1982) Somatic sensory transmission to the cortex during movement: gating of single cell responses to touch. Exp Neurol 78: 654 - 669.

Chapman CE, Jiang W, Lamarre Y (1988) Modulation of lemniscal input during conditioned arm movements in the monkey. Exp Brain Res 72: 316 - 334.

Cohen DAD, Prud'Homme MJL, Kalaska JF (1994) Tactile activity in primate primary somatosensory cortex during active arm movements: Correlation with receptive field properties. J Neurophysiol 71: 161 - 172.

Colburn TR, Evarts EV (1978) Long-loop adjustments during intended movements: Use of brushless DC torque motors in studies of neuromuscular function. In: Desmedt JE (ed), Progress in Clinical Neurophysiology, Vol 4. Karger, New York, pp. 153 - 166.

Coquery J-M (1978) Role of active movements in control of afferent input from skin in cat and man. In: Gordon G (ed), Active touch: The mechanisms of object manipulation: A multidisciplinary approach. Pergamon, Oxford, pp. 161 - 169.

Cowan RL, Wilson CJ (1994) Spontaneous firing patterns and axonal projections of single corticostriatal neurons in rat medial agranular cortex. J Neurophysiol 71: 17 - 31.

Dyhre-Poulsen P (1978) Perception of tactile stimuli before ballistic and during tracking movements. In: Gordon G (ed), Active touch: The mechanisms of object manipulation: A multidisciplinary approach. Pergamon, Oxford, pp. 171 - 176.

Dykes RW, Landry P, Metherate R, Hicks TP (1984) Functional role of GABA in cat primary somatosensory cortex: shaping receptive fields of cortical neurons. J Neurophysiol 52: 1066 - 1093

Eckhorn R, Bauer R, Jordan W, Brosch M, Kruse W, Munk M, Reitboeck HJ (1988) Coherent oscillations: A mechanism of feature linking in the visual cortex? Biol Cybern 60: 121 - 130.
Ellaway PH (1977) An application of cumulative sum technique (cusums) to neurophysiology. J Physiol (Lond) 265: 1 - 2P.
Engel AK, König P, Kreiter AK, Schillen TB, Singer W (1992) Temporal coding in the visual cortex: New vistas on integration in the nervous system. Trends in Neurosci 15: 218 - 226.
Evarts EV (1966) Methods for recording activity of individual neurons in moving animals. In: Rushmer RF (ed), Methods in medical research. Vol 2. Yearbook, Chicago, pp. 241 - 250.
Ghose GM, Freeman RD (1992) Oscillatory discharge in the visual system: Does it have a functional role? J Neurophysiol 68: 1558 - 1574.
Gray CM (1994) Synchronous oscillations in neuronal systems: Mechanisms and functions. J Comput Neurosci 1: 11 - 38.
Gray CM, Engel AK, König P, Singer W (1991) Mechanisms underlying the generation of neuronal oscillations in cat visual cortex. In: Basar E, Bullock TH (eds), Induced rhythmicities in the brain. Birkhauser, Boston, pp. 29 - 45.
Gray CM, Singer W (1989) Stimulus-specific neuronal oscillations in orientation columns of cat visual cortex. Proc Natl Acad Sci USA 86: 1698 -1702.
Hendry SHC, Jones EG, Emson PC, Lawson DEM, Heizmann CW, Streit P (1989) Two classes of cortical GABA neurons defined by differential calcium binding protein immunoreactivities. Exp Brain Res 76: 467 - 472.
Horowitz P, Hill W (1980) The Art of Electronics. Cambridge Univ Press, Cambridge.
Istvan PJ, Zarzecki P (1994) Intrinsic discharge patterns and somatosensory inputs for neurons in racoon primary somatosensory cortex. J Neurophysiol 72: 2827 - 2836.
Jagadeesh B, Gray CM, Ferster D (1992) Visually evoked oscillations of membrane potential in cells of cat visual cortex. Science 257: 552 - 554
Jiang W, Chapman CE, Lamarre Y (1991) Modulation of the cutaneous responsiveness of neurons in the primary somatosensory cortex during conditioned arm movements in the monkey. Exp Brain Res 84: 342 - 354.
Jones EG (1975) Varieties and distribution of non-pyramidal cells in the somatic sensory cortex of the squirrel monkey. J Comp. Neurol 160: 205 - 268.
Jones EG (1986) Connectivity of the primate sensory-motor cortex. In: Jones EG, Peters A (eds), Cerebral Cortex. Vol. 5. Sensory-Motor Areas and Aspects of Cortical Connectivity. Plenum Press, New York and London, pp. 113 - 183.
Kawaguchi Y (1993) Groupings of nonpyramidal and pyramidal cells with specific physiological and morphological characteristics in rat frontal cortex. J Neurophysiol 69: 416 - 431.
Kawaguchi Y, Kubota Y (1993) Correlation of physiological subgroupings of nonpyramidal cells with parvalbumin$_{D28k}$ - immunoreactive neurons in layer V of rat frontal cortex. J Neurophysiol 70: 387 - 395.
Lebedev MA, Denton JM, Nelson RJ (1994) Vibration-entrained and premovement activity in monkey primary somatosensory cortex. J Neurophysiol 72: 1654 - 1673.
Lebedev MA, Nelson RJ (1993) Modulation of rhythmic firing of monkey primary somatosensory cortical (SI) and neostriatal (NS) neurons during active hand movements. (319.8). Society for Neuroscience Abstracts 19: 781.
Lemon R (1984) Methods for Neuronal Recording in Conscious Animals. IBRO handbook series: Methods in the neurosciences. Vol 4. John Wiley & Sons, Chichester, UK.
Llinas RR (1990) Intrinsic electrical properties of nerve cells and their role in network oscillation. Cold Spring Harb Symp on Quant Biol 55: 933 - 938.
Llinas RR, Grace AA, Yarom Y (1991) In vitro neurons in mammalian cortical layer 4 exhibit intrinsic oscillatory activity in the 10- to 50-Hz frequency range. Proc Natl Acad Sci USA 88: 897 - 901.
Lopes da Silva F (1991) Neural mechanisms underlying brain waves: From neural membranes to networks. Electroenceph clin Neurophysiol 79: 81 - 93.
Lytton WW, Sejnowski TJ (1991) Simulations of cortical pyramidal neurons synchronized by inhibitory interneurons. J Neurophysiol 66: 1059 - 1079

McCormick DA, Connors BW, Lighthall JW, Prince DA (1985) Comparative electrophysiology of pyramidal and sparsely spiny stellate neurons of the neocortex. J Neurophysiol 54: 782 - 806.
Mountcastle VB, Talbot WH, Sakata H, Hyvärinen J (1969) Cortical neuronal mechanisms in flutter-vibration studies in unanesthetized monkeys: Neuronal periodicity and frequency discrimination. J Neurophysiol 32: 452 - 484.
Mountcastle VB, Steinmetz, MA, Romo R (1990) Frequency discrimination in the sense of flutter: Psychophysical measurements correlated with postcentral events in behaving monkeys. J Neurosci 10: 3032 - 3044.
Murthy VN, Fetz EE (1992) Coherent 25- to 35-Hz oscillations in the sensorimotor cortex of awake behaving monkeys. Proc Natl Acad Sci USA 89: 5670 - 5674.
Murthy VN and Fetz EE (1994) Synchronization of primate sensorimotor cortex neurons during 20 - 40 Hz field potential oscillations. (403.16). Society for Neuroscience Abstracts 20: 984.
Nelson RJ (1987) Activity of monkey primary somatosensory cortical neurons changes prior to active movement. Brain Res 406: 402 - 407.
Nelson RJ (1988) Set related and premovement related activity of primate somatosensory cortical neurons depends upon stimulus modality and subsequent movement. Brain Res Bull 21:411 - 424.
Nelson RJ, Smith BN, Douglas VD (1991) Relationship between sensory responsiveness and premovement activity of quickly adapting neurons in areas 3b and 1 of monkey primary somatosensory cortex. Exp Brain Res 84: 75 - 90.
Nuñez A, Amzica F, Steriade M (1992) Voltage-dependent fast (20 - 40 Hz) oscillations in long-axoned neocortical neurons. Neuroscience 51: 7 - 10.
Perkel DH, Gerstein G, Moore G (1967) Neuronal spike trains and stochastic point processes. I. The single spike train. Biophys J 7: 391 - 418.
Poggio T, Viernstein L (1964) Time series analysis of impulse sequences of thalamic somatic sensory neurons. J Neurophysiol 27: 517 - 545.
Prochazka A (1985) Proprioception during movement. Can J Physiol Pharmacol 64: 499-504.
Ramón y Cajal S (1911) Histologie du Système Nerveux de l'Homme et des Vertébrés. Vol. 2. Maloine, Paris.
Rodieck RW, Kiang NY-S, Gerstein GL (1962) Some quantitative methods for the study of spontaneous activity of single neurons. Biophys. J. 2: 351 - 368.
Rougeul A, Bouer JJ, Dedet L, Debray O (1979) Fast somato-parietal rhythms during combined focal attention in baboon and squirrel monkey. Electroenceph Clin Neurophysiol 46: 310 - 319.
Rushton DN, Rothwell JC, Graggs MD (1981) Gating of somatosensory evoked potentials during different kinds of movement in man. Brain 104: 465 - 491.
Sanes JN, Donoghue JP (1993) Oscillations in local field potentials of the primate motor cortex during voluntary movements. Proc Natl Acad Sci USA 90: 4470 - 4474.
Segundo JP, Perkel DH, Wyman H, Hegstad H, Moore GP (1968) Input-output relations in computer-simulated nerve cells. Influence of the statistical properties, strength, number and inter-dependence of excitatory pre-synaptic terminals. Kibernetic 4: 157 - 171.
Sheer DE (1989) Sensory and cognitive 40-Hz event-related potentials: Behavioral correlates, brain function, and clinical applications. In: Basar E, Bullock TH (eds) Springer series in brain dynamics 2. Springer-Verlag, Berlin, Heidelberg, pp. 339 - 374.
Siebler M, Köller H, Rose G, Müller HW (1991) An improved graphical method for pattern recognition from spike trains of spontaneously active neurons. Exp Brain Res 90: 141-146.
Silva LR, Amitai Y, Connors BW (1991) Intrinsic oscillations of neocortex generated by layer 5 pyramidal neurons. Science 251: 432 - 435.
Singer W (1993) Synchronization of cortical activity and its putative role in information processing and learning. Annu Rev Physiol 55: 349 - 374.
Softky WR, Koch C (1993) The highly irregular firing of cortical cells is inconsistent with temporal integration of random EPSPs. J Neurosci 13: 334 - 350.

Somogyi P, Cowey A (1981) Combined Golgi and electron microscopic study on the synapses formed by double bouquet cells in the visual cortex of the cat and monkey. J Comp Neurol 195: 547 - 566.
Soso MJ, Fetz EE (1980) Responses of identified cells in postcentral cortex of awake monkeys during comparable active and passive joint movements. J Neurophysiol 43: 1090 - 1110.
Steriade M (1993) Central core modulation of spontaneous oscillations and sensory transmission in thalamocortical systems. Curr Opin Neurobiol 3: 619 - 625.
Stern EA, Wilson CJ (1994) High-frequency activity in the depolarized state of corticostriatal and striatal neurons. (238.12). Society for Neuroscience Abstracts 20: 565.
Surmeier DJ, Towe AL (1987a) Properties of proprioceptive neurons in the cuneate nucleus of the cat. J Neurophysiol 57: 938 - 961.
Surmeier DJ, Towe AL (1987b) Intrinsic features contributing to spike train patterning in proprioceptive cuneate neurons. J Neurophysiol 57: 962 - 976.
Vaadia E, Kurata K, Wise, SP (1988) Neuronal activity preceding directional and nondirectional cues in the premotor cortex of rhesus monkeys. Somatosensory and Motor Research 6: 207 - 230.
White EL (1989) Cortical Circuits: Synaptic Organization of the Cerebral Cortex: Structure, Function and Theory. Birkhäuser, Boston, MA.
Wiesendanger M, Miles TS (1982) Ascending pathway of low-threshold muscle afferents to the cerebral cortex and its possible role in motor control. Physiol Rev 62: 1234 - 1270.
Wilson CJ, Groves PM (1981) Spontaneous firing patterns of identified spiny neurons in the rat neostriatum. Brain Res 220: 67 - 80.
Wilson FAW, Scalaidhe SPÓ, Goldman-Rakic PS (1994) Functional synegism between putative γ-aminobutyrate-containing neurons and pyramidal neurons in prefrontal cortex. Proc Natl Acad Sci USA 91: 4009 - 4013.
Wilson CJ, Young SJ, Groves PM (1977) Statistical properties of neuronal spike trains in the substantia nigra: cell types and their interactions. Brain Res. 136: 243 - 260.
Zadeh LA (1957) Signal-flow graphs and random signals. Proc IRE 45:1413 - 1414.

Figure Legends

Fig. 1. Schematics of the manipulandum, the feedback display, and the task. A: Apparatus for studying wrist movements. B: Visual display of wrist position that consisted of light-emitting diodes. C: Diagram of experimental paradigm.

Fig. 2. Cortical locations of rhythmically firing SI neurons. A: A drawing of the dorsolateral view of the brain. Central sulcus (CS) and intraparietal sulcus (IPS) are indicated. B: A table showing the number of rhythmically firing neurons by receptive field (RF) type recorded in each SI region (areas 3a, 3b, 1, and 2). C: Locations of recording sites for six monkeys. The illustration for each monkey consists of four panels. The top panel presents a surface map of electrode penetrations with respect to CS and IPS. The penetrations where rhythmically firing neurons were recorded are indicated by larger marks. The lower panels illustrate three sagittal sections through the cortex (lateral, intermediate, and medial). Locations of the neurons are shown as projections to the nearest of the three sections. RF types are marked according to the convention of panel B.

Fig. 3. Selection of the group of rhythmically firing neurons. A: A computer-generated example of an expectation density (ED) histogram. The spike train constructed to have a normal distribution of interspike intervals corresponding to 30 Hz and a coefficient of variation of 0.15. R is the stabilized level of the histogram, E_1, E_2 are the heights, and t_1, t_2 are the times of the initial two peaks. B: Histograms of the distribution of the ratio of the first peak to stabilized ED level (E_1 / R) for rhythmically firing and nonrhythmically firing neurons. C-D: scattergrams illustrating selection of rhythmically firing neurons based on the heights of ED peaks and the jitter of first interpeak interval. Jitter is the time of the first peak minus the time between the first and second

peaks divided by the time of the first peak. E: Histogram of the distribution of the firing frequency for the total sample of rhythmically firing SI neurons.

Fig. 4. Analyses of rhythmic activity (~39 Hz; same records as in Fig. 5). Spike trains for the hold period (500 ms epoch preceding vibration onset) were analyzed. A: Hold period interspike interval (ISI) scattergram for 40 consecutive trials. Each column represents a trial. B: Joint interval scattergram. C: ISI distribution histogram. D: Expectation density histogram. E: Renewal density histogram. In panels C - E, bin width is 1 ms.

Fig. 5. Example of changes in neuronal activity associated with 57 Hz vibratory go-cue presentation and movement. Records in the left parts of panels A - E are centered on vibration onset, whereas those in the right parts are centered on movement onset. The activity pattern of a rhythmically firing (~39 Hz) area 1 neuron exhibited during flexion trials is illustrated. A: Raster displays of interspike intervals (ISIs). For each spike, these displays show the time of its occurrence on the x-axis and plot the next ISI on the y-axis. B: Histograms of discharge rate (bin width = 5 ms). Dotted lines represent average movement onset (left panel) and average vibration onset (right panel). C: Raster displays of discharges. Each horizontal line corresponds to one trial, and each dot represents the time of a spike's occurrence. Bold marks indicate movement onsets (on the left) and vibration onsets (on the right). The trials were rearranged in the order of increasing reaction time from top to bottom. D: Plots of the average cumulative sum (CUSUM). The time of statistically significant deviations of the CUSUM trace are shown. E: Average wrist position traces. F: A schematic illustration of the neuron's receptive field (RF). This neuron had a noncutaneous RF deeply located in the hand. G: Cortical location of the neuron.

Fig. 6. Examples of characteristics of rhythmic spike trains that seem unlikely for a renewal mechanism of rhythm generation. A - D: Records for a rhythmically firing (~43 Hz) area 1 neuron with a multimodal ISI distribution. A: Activity during task performance (conventions as in Fig. 5). B: Analyses of rhythmic activity during the hold period (conventions as in Fig. 4). C: Receptive field (RF) schematic. This neuron had a cutaneous RF located on the second digit. D: Cortical location of the neuron. E - H: Records for an area 3b neuron that had interrupting spikes. E: Activity during task performance (conventions as in Fig. 5). F: Analyses of rhythmic activity during the hold period (conventions as in Fig. 4). G: No clear RF was found for this neuron. H: Cortical location of the neuron.

Fig. 7. Analyses of the changes in activity of a rhythmically firing (~30 Hz) neuron occurring after vibratory go-cue presentation. A: A typical example of vibration-related changes in activity (conventions as in Fig. 5). The frequency of vibration was 57 Hz. B: A schematic illustration of the neuron's receptive field (RF). This neuron was activated by passive extension of the fourth digit at the metacarpophalangeal joint. C: The neuron's cortical location. D: Analyses of the rhythmic activity during the hold period (conventions as in Fig. 4). E: A schematic illustration of the typical pattern of activity modulation by vibration. F. Frequency distribution histogram of latencies of responses to 57 Hz vibratory stimulation (the most extensively studied frequency).

Fig. 8. An example of entrainment of neuronal activity to the frequency of a vibratory stimulus. A: Records for a rhythmically firing (~30 Hz) area 3a neuron (conventions as in Fig. 5). The frequency of vibration was 27 Hz. B: Phase raster. C: Receptive field schematic. The neuron was activated by passive wrist extension. D: The neuron's cortical location. E: Analyses of rhythmic activity during the hold period (conventions as in Fig. 4). F: Analyses of activity for the epoch of sustained vibratory response (100 - 400 ms after vibration onset). Conventions as in Fig. 4. Expectation and renewal density histograms were not calculated because the duration of the movement associated activity burst was too short to derive meaningful displays. G: Distribution of discharges over the vibratory cycle. The vibratory stimulus is illustrated by the sinusoidal trace. Upward deviations of this trace corresponds to upward movements of the manipulandum. Expectation and renewal density histograms were not calculated because the duration of the movement associated activity burst was too short to derive meaningful displays.

Fig. 9. A typical example of premovement activity (PMA. A: Records for a rhythmically firing (~44 Hz) area 2 neuron (conventions as in Fig. 5). Vibratory frequency was 57 Hz. B: No clear receptive field was found for this neuron. C: The neuron's cortical location. D: Analyses of rhythmic activity during the hold period (conventions as in Fig. 4). E: A schematic illustration of the typical PMA pattern, i.e., an activity decrease. F: The frequency distribution histogram of PMA onsets with respect to movement onset and adjusted earliest and average EMG onset (see text).

Fig. 10. Transition of neuronal activity from a rhythmic to a nonrhythmic pattern during movement. A: Records for a rhythmically firing (~28 Hz) area 1 neuron (conventions as in Fig. 5). B: Receptive field schematic. This neuron was activated by passive extension of the second digit at the metacarpophalangeal joint. C: The neuron's cortical location. D: Analyses of rhythmic activity during the hold period (conventions as in Fig. 4). E: Analyses of activity occurring with movement (50 - 150 ms with respect to movement onset. Conventions as in Fig. 4. Full scale for ISI histogram is 80 ms. Expectation and renewal density histograms were not calculated because the duration of the movement associated activity burst was too short to derive meaningful displays.

Fig. 11. Comparison of the activity patterns seen during flexion and extension trials. Records for a rhythmically firing (~38 Hz) area 3a neuron are shown. Vibratory frequency was 57 Hz A: Records for flexion trials (conventions as in Fig. 5). B: Analyses of rhythmic activity for the hold period during flexion trials (conventions as in Fig. 4). C: Schematic illustration of the neuron's cortical location. D: Records for extension trials. E: Analyses of rhythmic activity for the hold period during extension trials.

Fig. 12. A model of rhythmically active SI neurons as tonic inhibitory interneurons that gate the activity of cortical output neurons. Synapses marked black represent inhibitory interactions, while those marked white represent excitation. Line thickness corresponds to the strength of the connections.

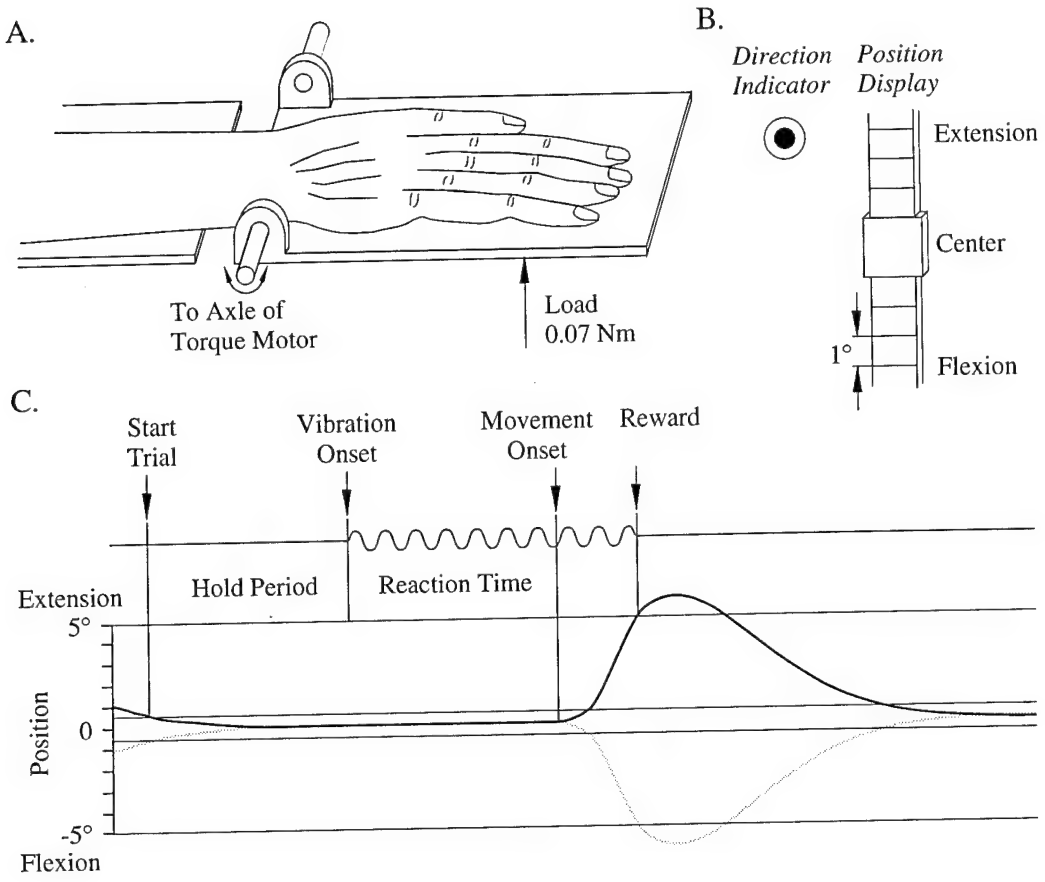
A.
To Axle of
Torque Motor
Load
0.07 Nm
B.
Direction
Indicator
Position
Display
Extension
Center
1°
Flexion
C.
Start
Trial
Vibration
Onset
Movement
Onset
Reward
Hold Period
Reaction Time
Extension
5°
Position
0
-5°
Flexion

Figure 1

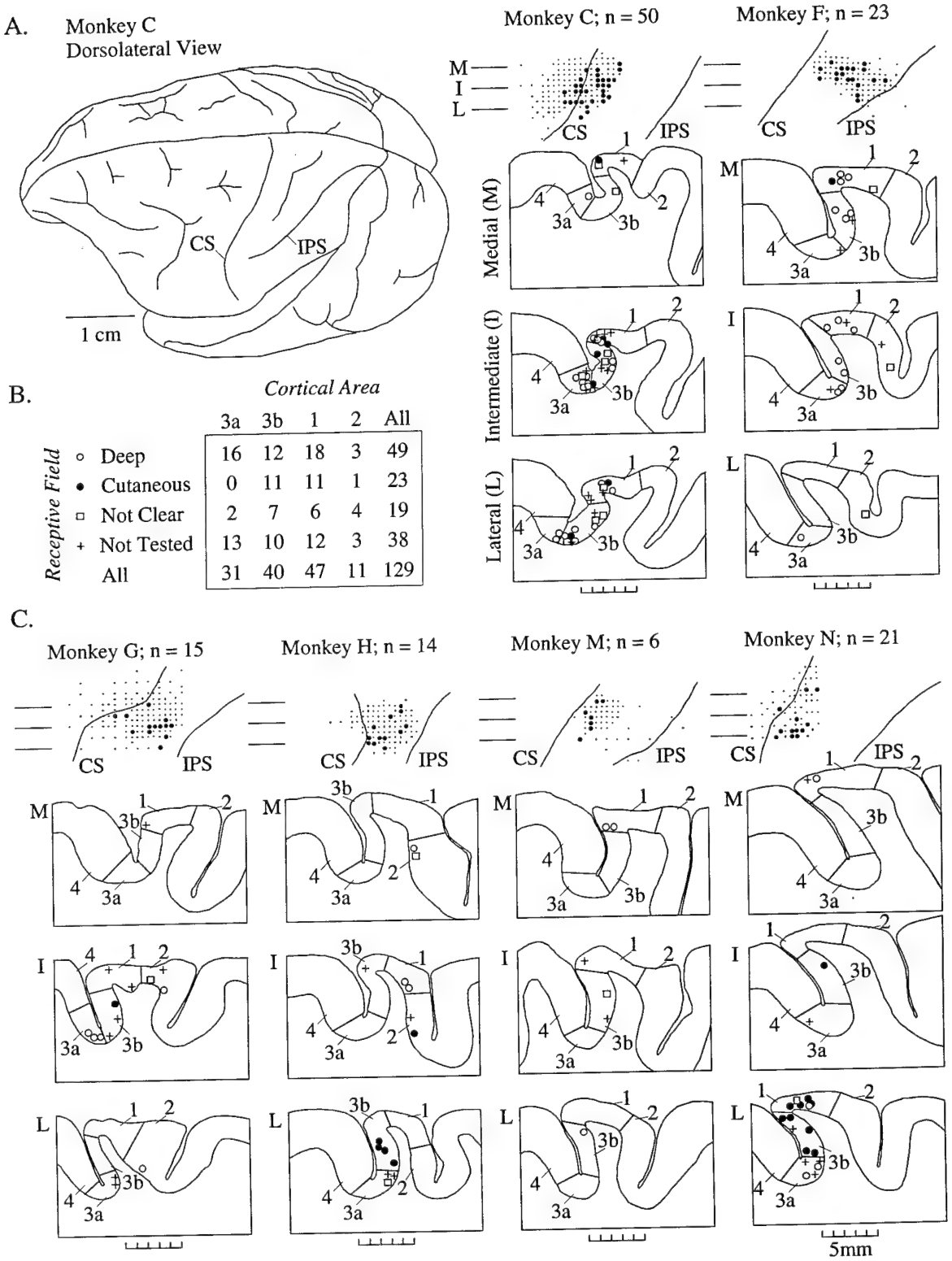
A.
Monkey C
Dorsolateral View
CS
IPS
1 cm
Monkey C; n = 50
Monkey F; n = 23
M
I
L
Medial (M)
Intermediate (I)
Lateral (L)
1
2
3a
3b
4
B.
Cortical Area
3a 3b 1 2 All
Receptive Field
Deep 16 12 18 3 49
Cutaneous 0 11 11 1 23
Not Clear 2 7 6 4 19
Not Tested 13 10 12 3 38
All 31 40 47 11 129
C.
Monkey G; n = 15
Monkey H; n = 14
Monkey M; n = 6
Monkey N; n = 21
5mm

Figure 2

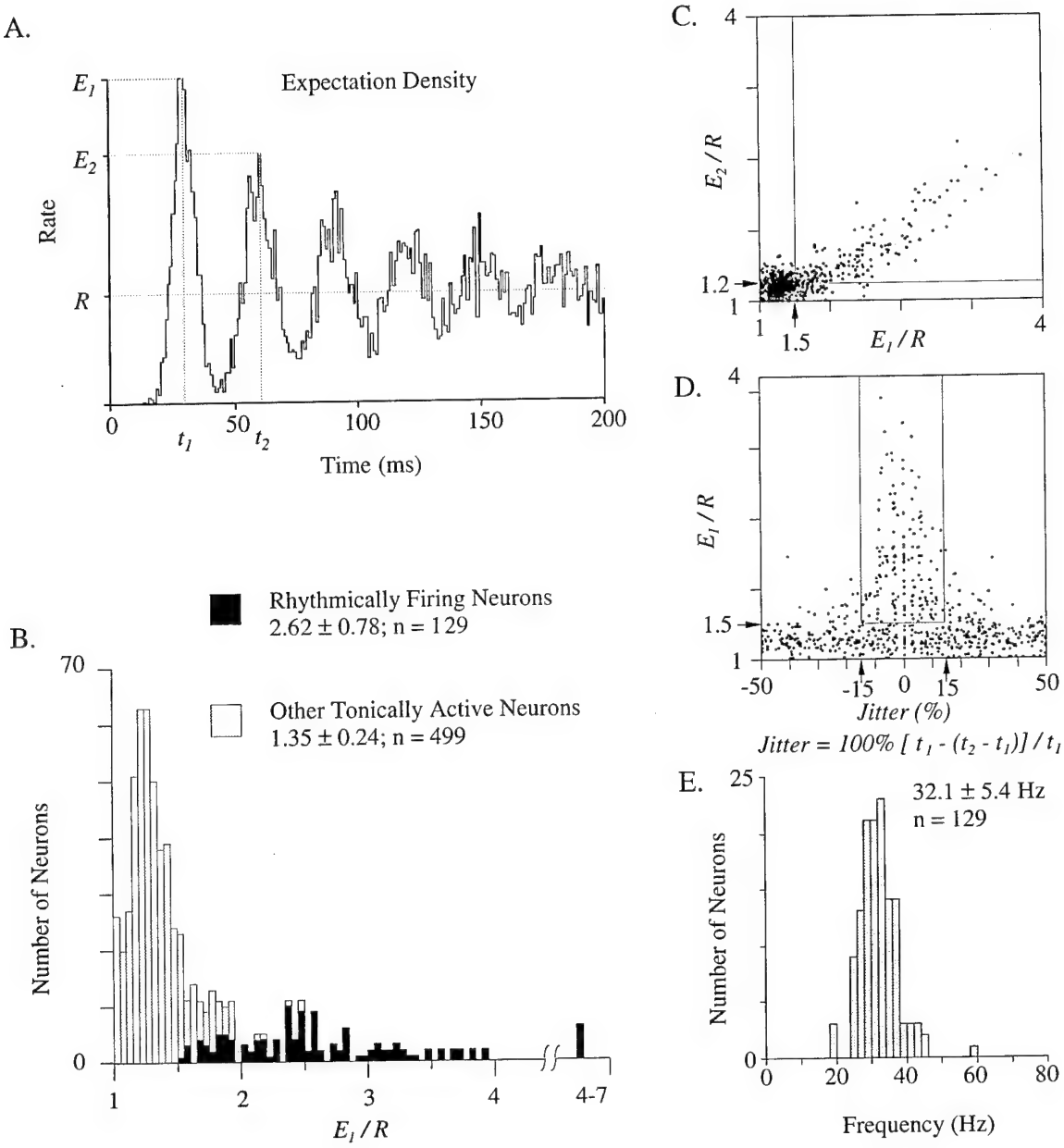
A.
Expectation Density
E_1
E_2
R
Rate
0
t_1
50
t_2
100
150
200
Time (ms)
B.
Rhythmically Firing Neurons
2.62 ± 0.78; n = 129
Other Tonically Active Neurons
1.35 ± 0.24; n = 499
70
0
Number of Neurons
1
2
3
4
4-7
E_1 / R
C.
4
E_2 / R
1.2
1
1
1.5
E_1 / R
4
D.
4
E_1 / R
1.5
1
-50
-15
0
15
50
Jitter (%)
Jitter = 100% [t_1 - (t_2 - t_1)] / t_1
E.
25
32.1 ± 5.4 Hz
n = 129
Number of Neurons
0
0
20
40
60
80
Frequency (Hz)

Figure 3

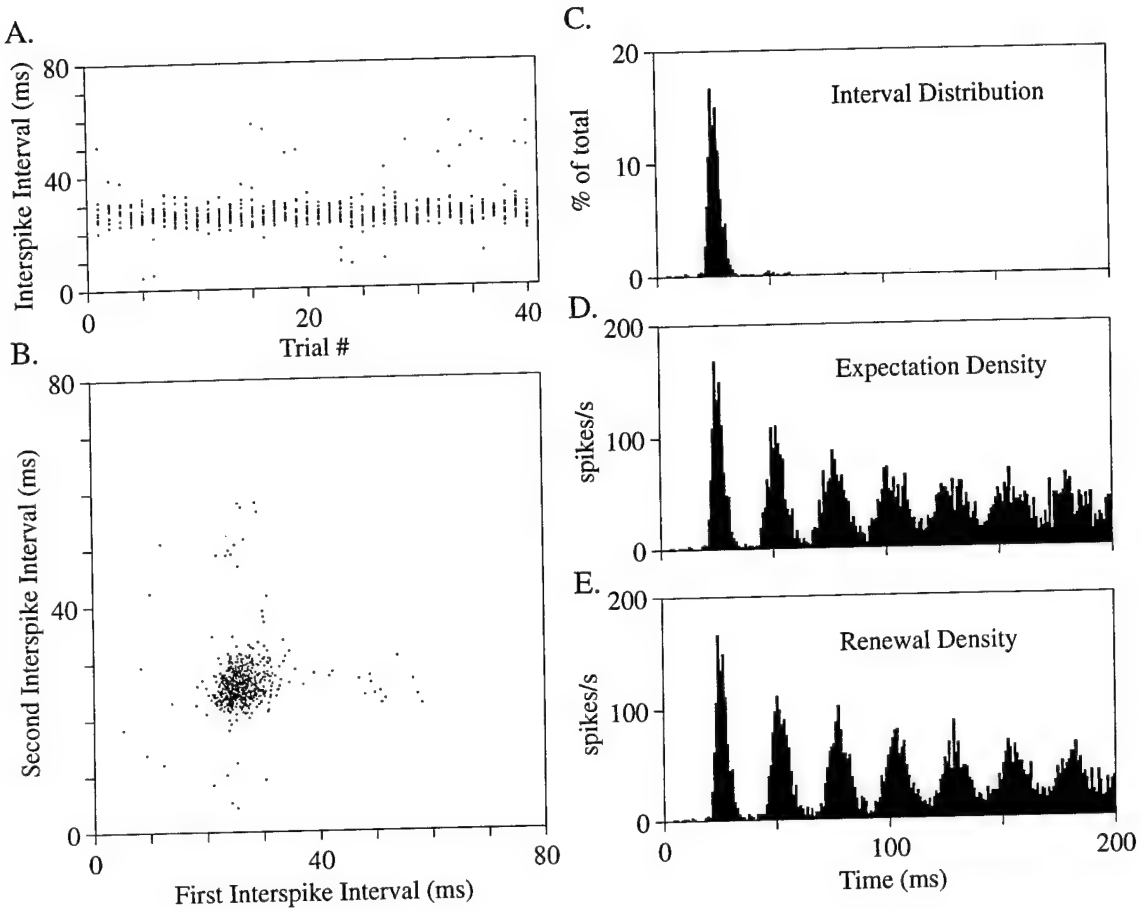
A.
Interspike Interval (ms)
80
40
0
0
20
40
Trial #
B.
Second Interspike Interval (ms)
80
40
0
0
40
80
First Interspike Interval (ms)
C.
Interval Distribution
% of total
20
10
0
D.
Expectation Density
spikes/s
200
100
0
E.
Renewal Density
spikes/s
200
100
0
0
100
200
Time (ms)

Figure 4

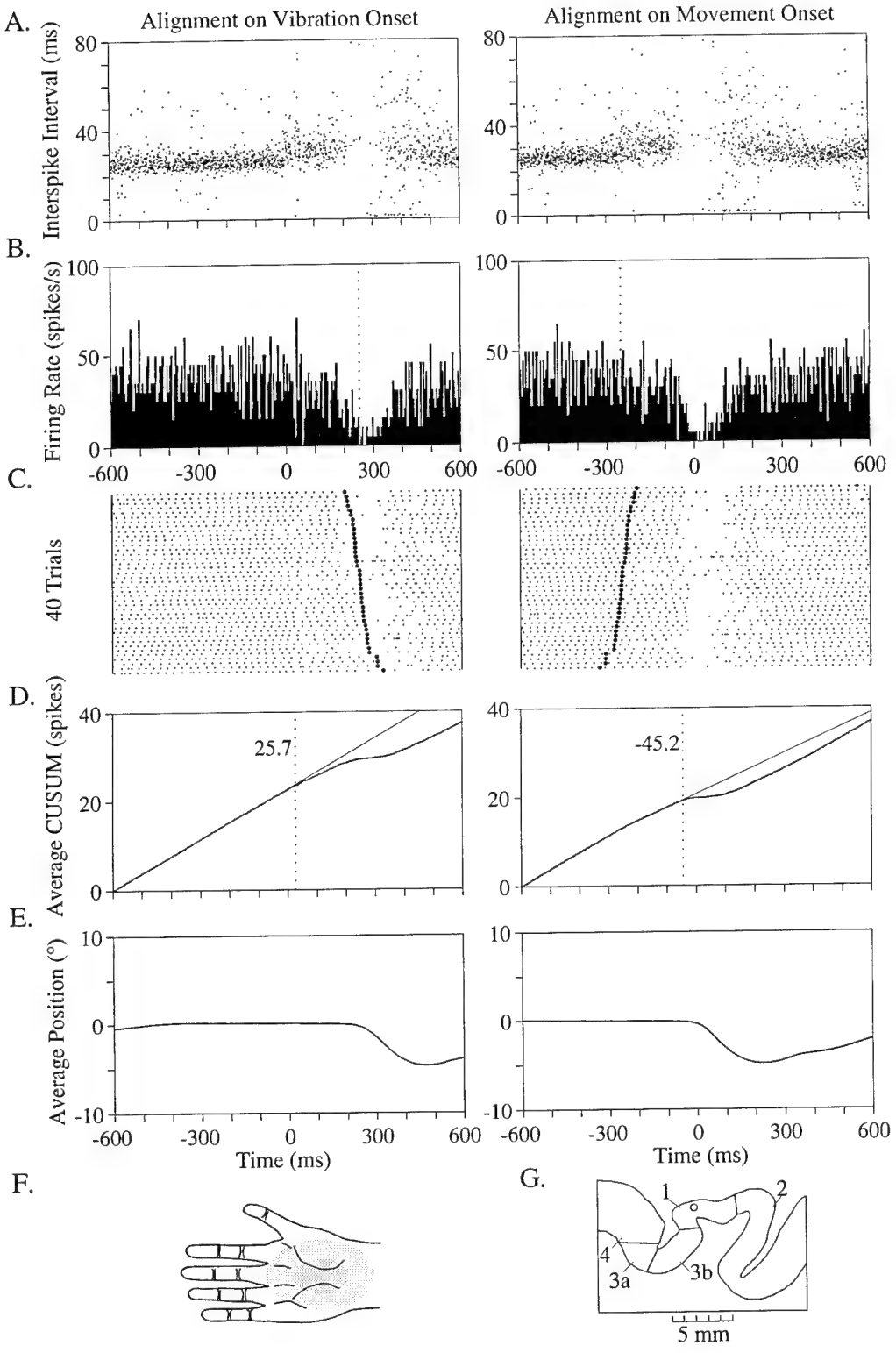
A.
Alignment on Vibration Onset
Alignment on Movement Onset
Interspike Interval (ms)
80
40
0
B.
Firing Rate (spikes/s)
100
50
0
-600
-300
0
300
600
C.
40 Trials
D.
Average CUSUM (spikes)
40
20
0
25.7
-45.2
E.
Average Position (°)
10
0
-10
Time (ms)
F.
G.
1
2
3a
3b
4
5 mm

Figure 5

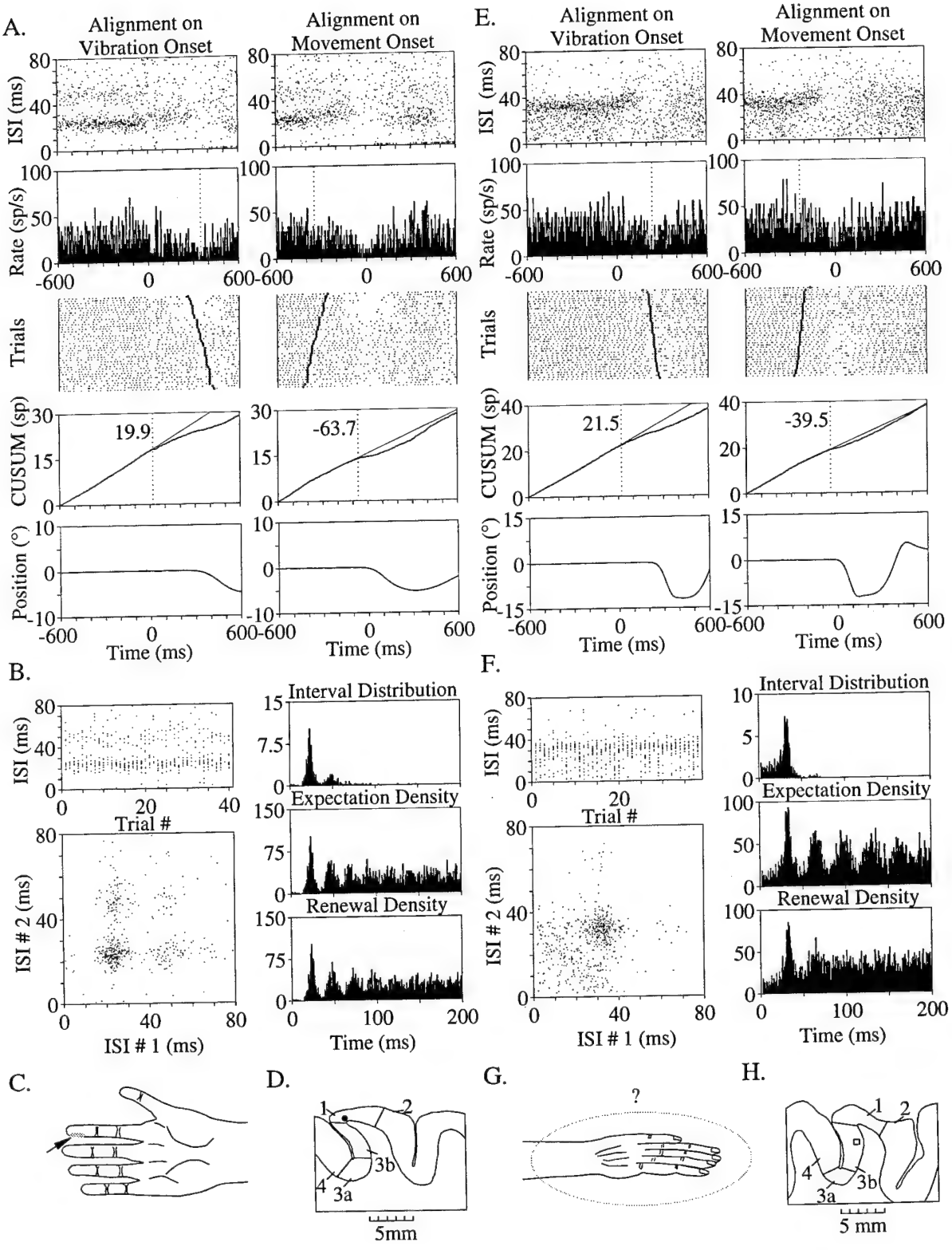
A.
Alignment on Vibration Onset
Alignment on Movement Onset
ISI (ms)
Rate (sp/s)
Trials
CUSUM (sp)
19.9
-63.7
Position (°)
Time (ms)
E.
Alignment on Vibration Onset
Alignment on Movement Onset
ISI (ms)
Rate (sp/s)
Trials
CUSUM (sp)
21.5
-39.5
Position (°)
Time (ms)
B.
ISI (ms)
Interval Distribution
Expectation Density
Trial #
ISI # 2 (ms)
Renewal Density
ISI # 1 (ms)
Time (ms)
F.
ISI (ms)
Interval Distribution
Expectation Density
Trial #
ISI # 2 (ms)
Renewal Density
ISI # 1 (ms)
Time (ms)
C.
D.
1
2
3b
4
3a
5mm
G.
?
H.
1
2
4
3b
3a
5 mm

Figure 6

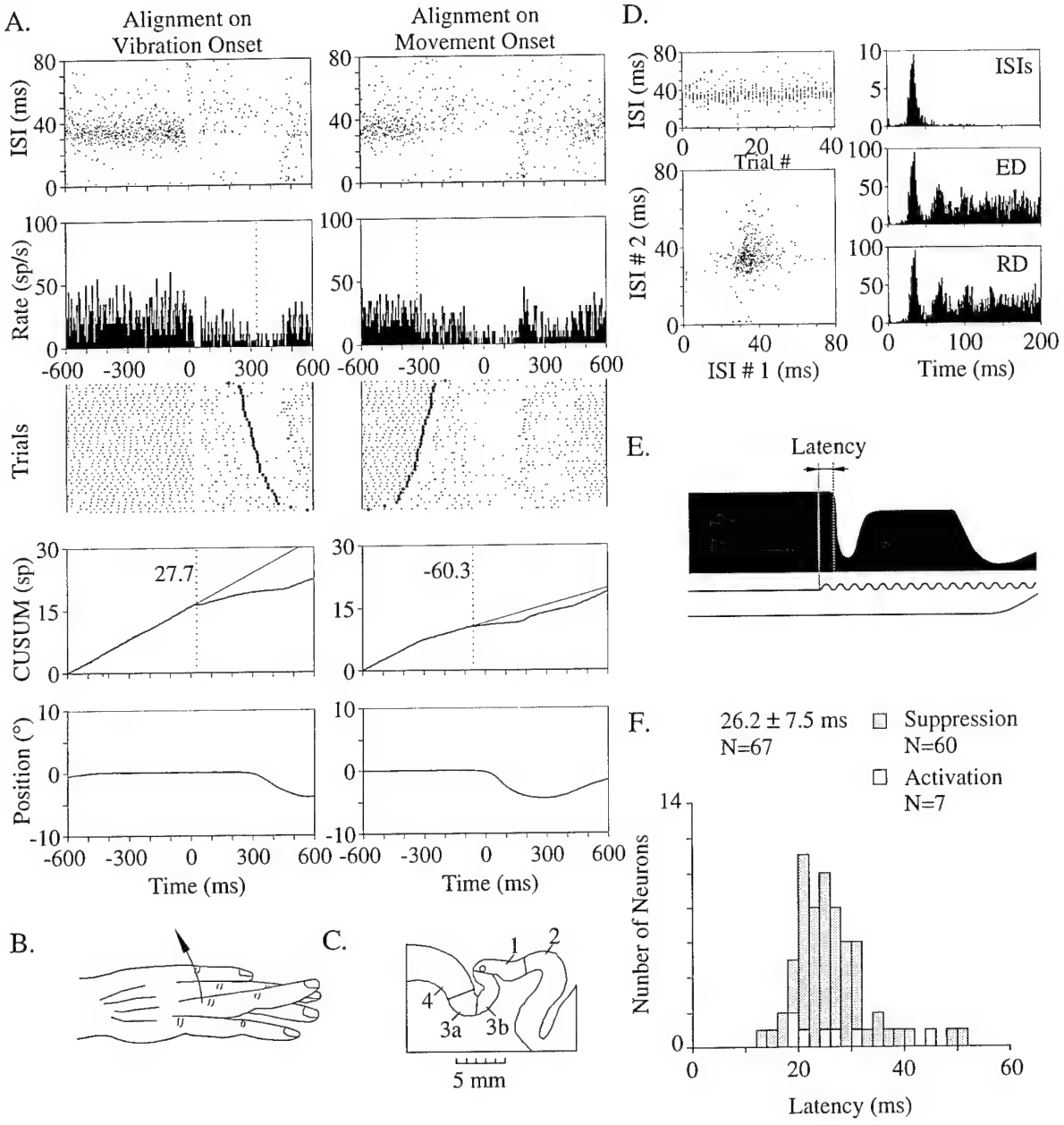
A.
Alignment on Vibration Onset
Alignment on Movement Onset
ISI (ms)
Rate (sp/s)
Trials
CUSUM (sp)
27.7
-60.3
Position (°)
Time (ms)
B.
C.
1
2
3a
3b
4
5 mm
D.
ISI (ms)
Trial #
ISI # 2 (ms)
ISI # 1 (ms)
ISIs
ED
RD
Time (ms)
E.
Latency
F.
26.2 ± 7.5 ms
N=67
Suppression
N=60
Activation
N=7
Number of Neurons
Latency (ms)

Figure 7

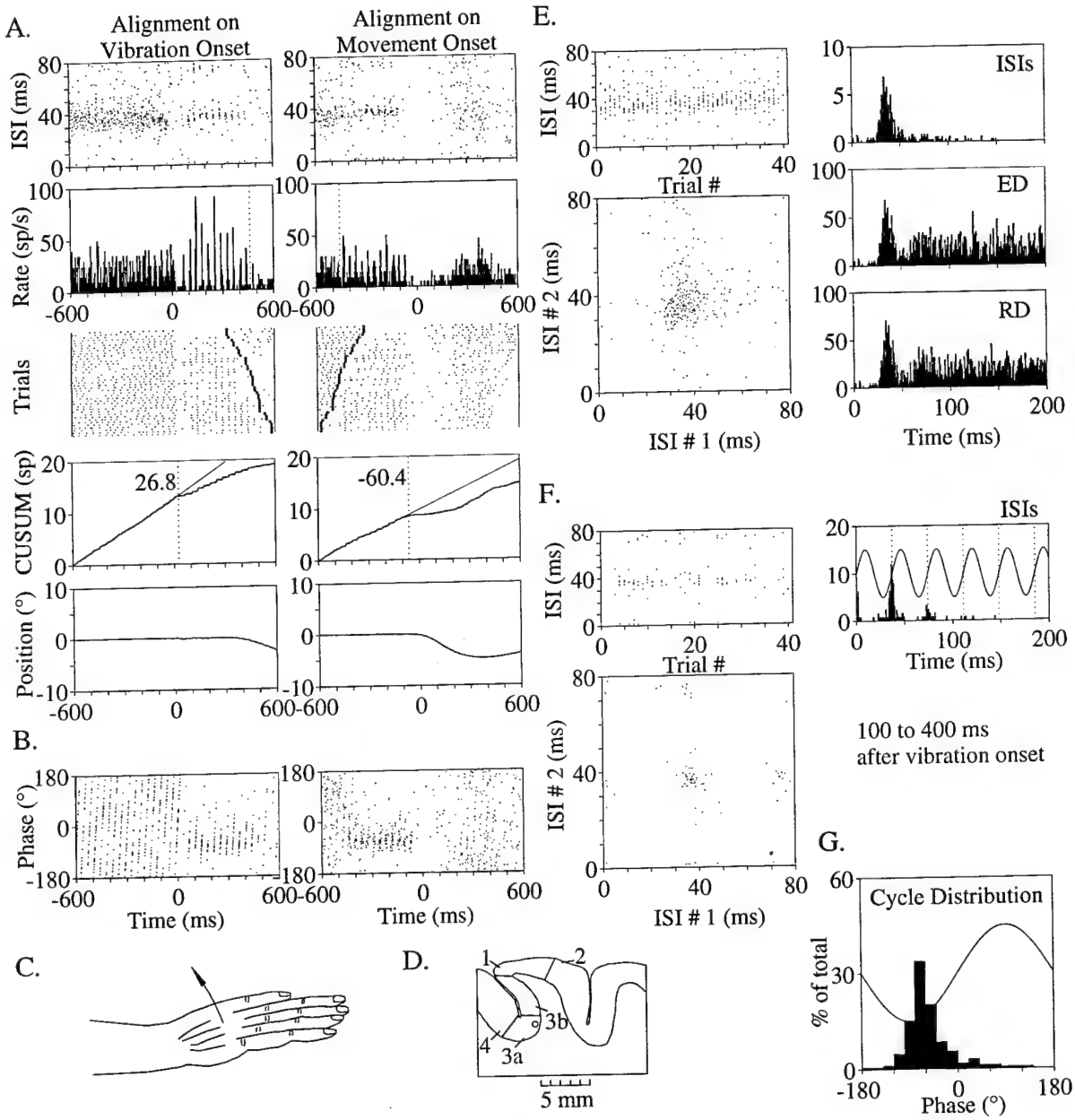
A.
Alignment on Vibration Onset
Alignment on Movement Onset
ISI (ms)
Rate (sp/s)
Trials
CUSUM (sp)
26.8
-60.4
Position (°)
B.
Phase (°)
Time (ms)
C.
D.
1
2
3b
4
3a
5 mm
E.
Trial #
ISI # 2 (ms)
ISI # 1 (ms)
ISIs
ED
RD
Time (ms)
F.
100 to 400 ms
after vibration onset
G.
Cycle Distribution
% of total
Phase (°)

Figure 8

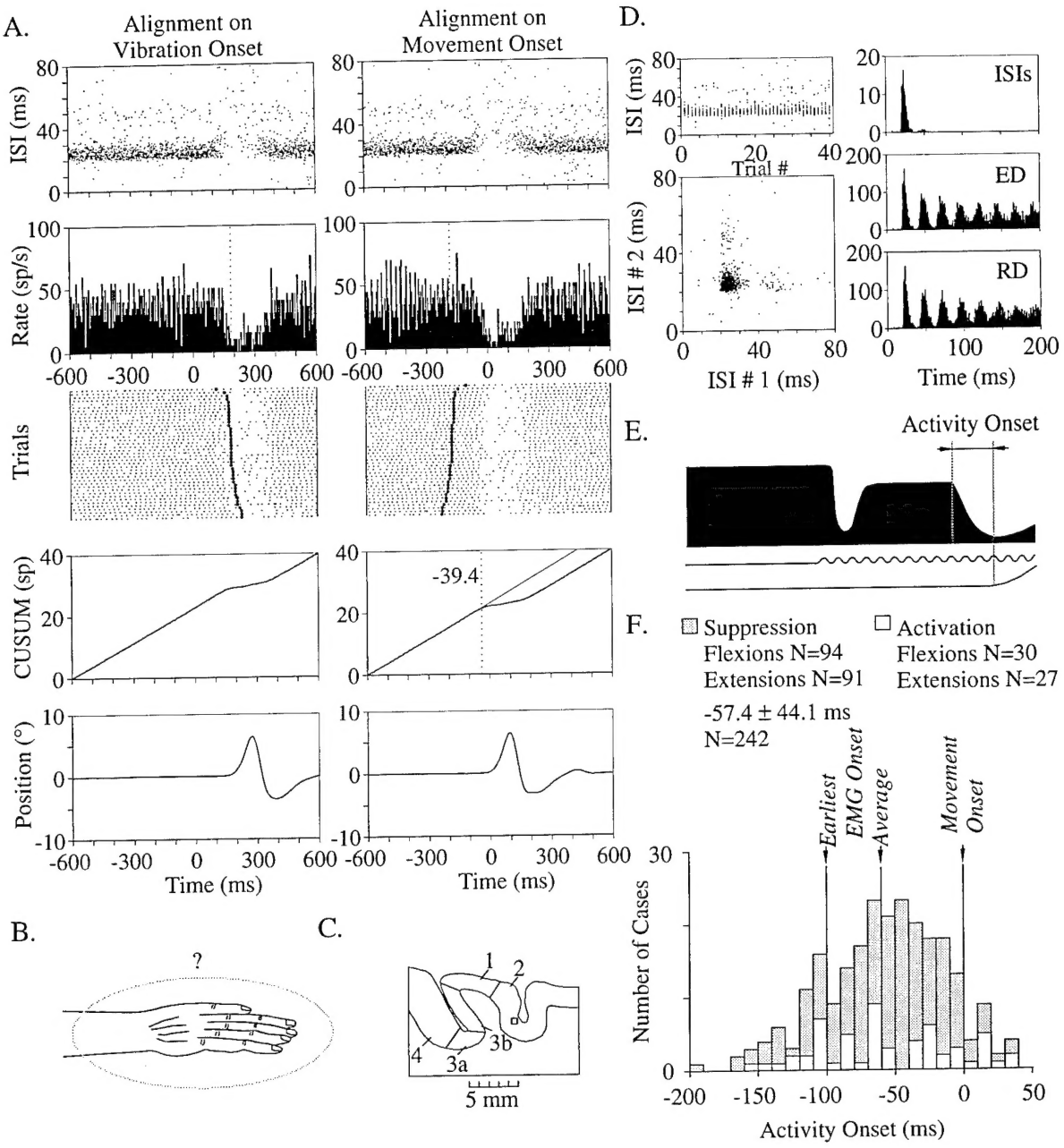
A.
Alignment on Vibration Onset
Alignment on Movement Onset
ISI (ms)
Rate (sp/s)
Trials
CUSUM (sp)
-39.4
Position (°)
Time (ms)
B.
?
C.
1
2
3b
4
3a
5 mm
D.
ISI (ms)
Trial #
ISI # 2 (ms)
ISI # 1 (ms)
ISIs
ED
RD
Time (ms)
E.
Activity Onset
F.
Suppression
Flexions N=94
Extensions N=91
Activation
Flexions N=30
Extensions N=27
-57.4 ± 44.1 ms
N=242
Earliest EMG Onset
Average
Movement Onset
Number of Cases
Activity Onset (ms)

Figure 9

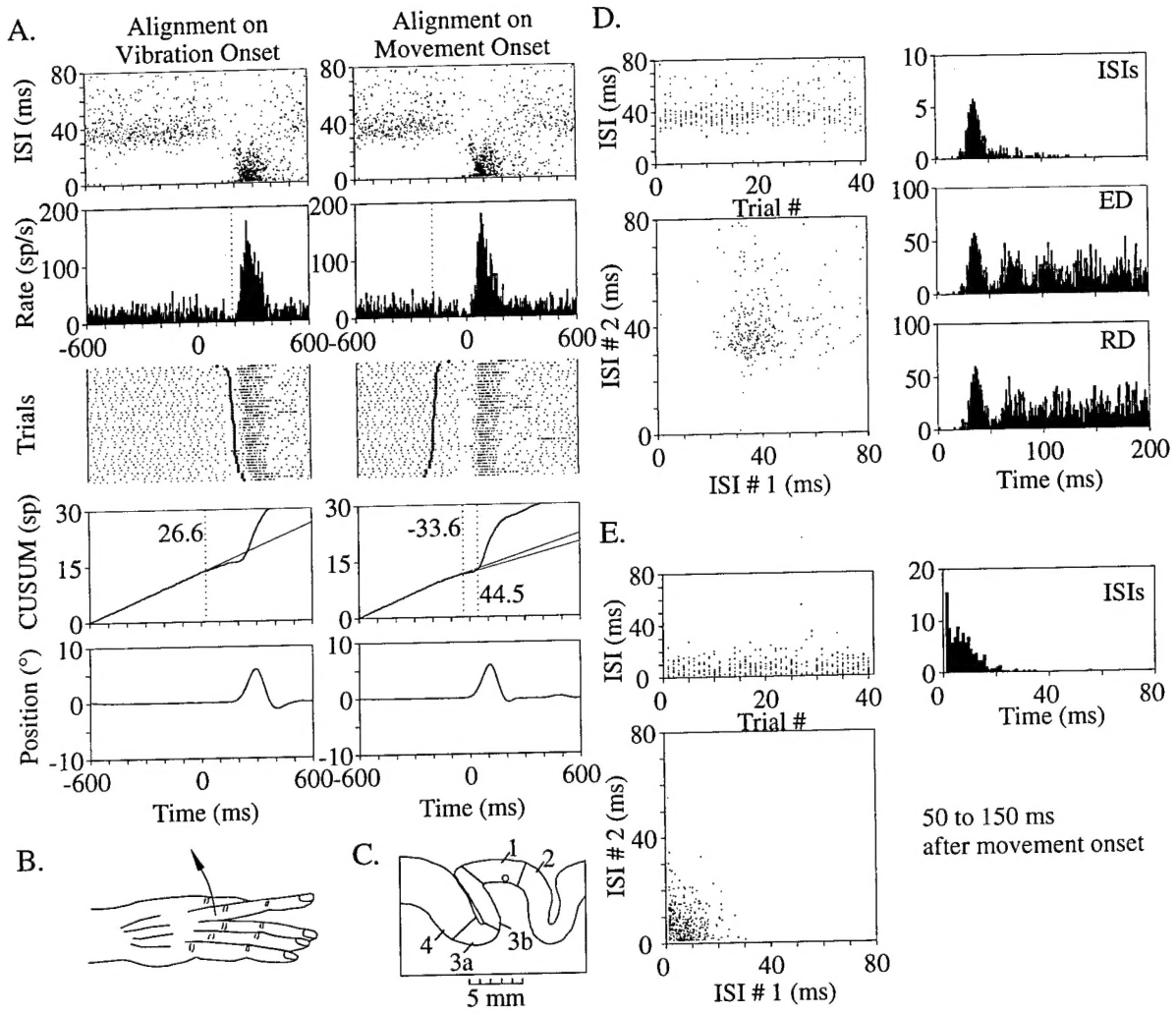
A.
Alignment on Vibration Onset
Alignment on Movement Onset
ISI (ms)
Rate (sp/s)
Trials
CUSUM (sp)
26.6
-33.6
44.5
Position (°)
Time (ms)
B.
C.
1
2
3b
4
3a
5 mm
D.
Trial #
ISI # 2 (ms)
ISI # 1 (ms)
ISIs
ED
RD
Time (ms)
E.
50 to 150 ms
after movement onset

Figure 10

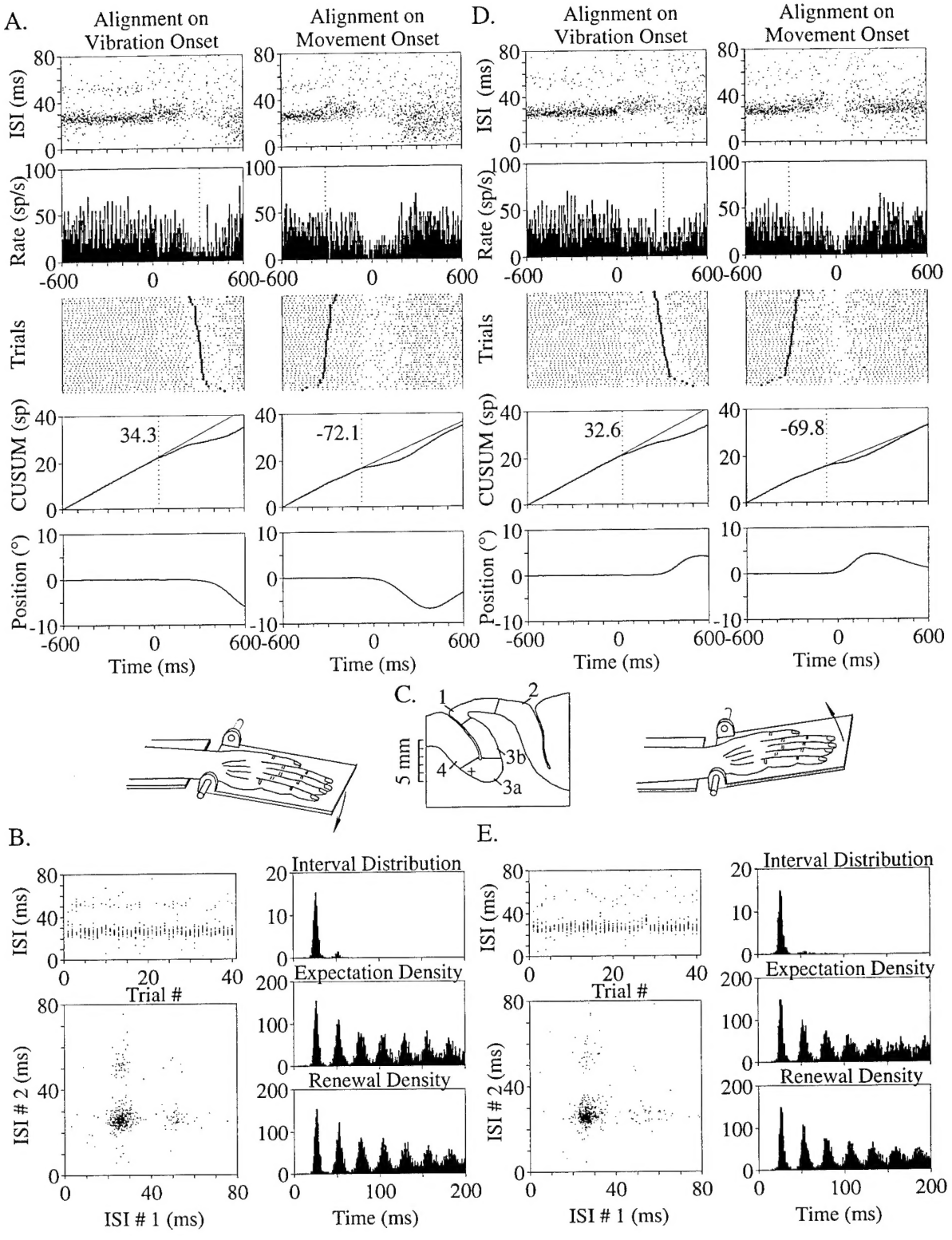
A.
Alignment on Vibration Onset
Alignment on Movement Onset
D.
Alignment on Vibration Onset
Alignment on Movement Onset
ISI (ms)
Rate (sp/s)
Trials
CUSUM (sp)
34.3
-72.1
32.6
-69.8
Position (°)
Time (ms)
C.
1
2
3b
4
3a
5 mm
B.
E.
Interval Distribution
Expectation Density
Renewal Density
Trial #
ISI # 2 (ms)
ISI # 1 (ms)

Figure 11

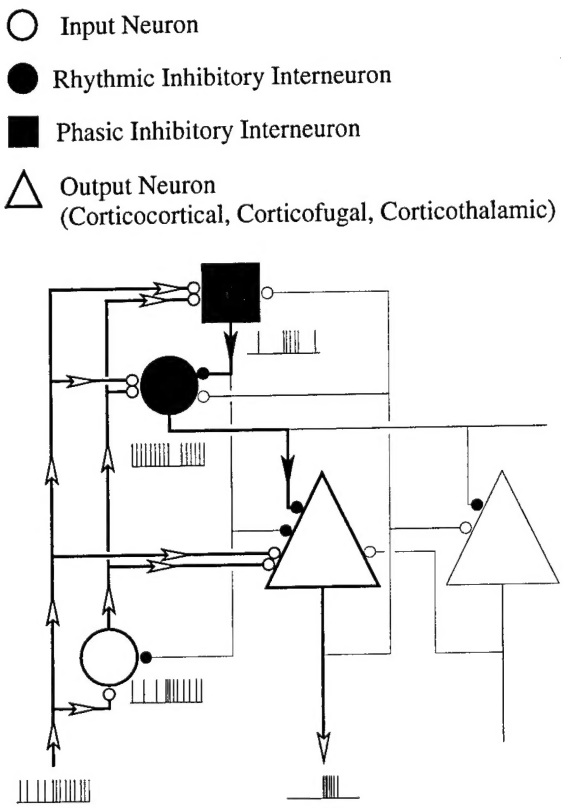
Input Neuron
Rhythmic Inhibitory Interneuron
Phasic Inhibitory Interneuron
Output Neuron
(Corticocortical, Corticofugal, Corticothalamic)

Figure 12